JBC RESEARCH ARTICLE

The circular RNA circNFIX regulates MEF2C expression in muscle satellite cells in spastic cerebral palsy

Received for publication, May 27, 2024, and in revised form, October 22, 2024 Published, Papers in Press, November 13, 2024,
https://doi.org/10.1016/j.jbc.2024.107987

Brigette Romero[1], Parsa Hoque[1], Karyn G. Robinson[2], Stephanie K. Lee[2], Tanvi Sinha[3], Amaresh Panda[3], Michael W. Shrader[2], Vijay Parashar[1], Robert E. Akins[2], and Mona Batish[1,*]

From the [1]Department of Medical and Molecular Sciences, University of Delaware, Newark, Delaware, USA; [2]Nemours Children's Research, Nemours Children's Health System, Wilmington, Delaware, USA; [3]Institute of Life Science (ILS), Nalco Square, Bhubaneswar, Odisha, India

Reviewed by members of the JBC Editorial Board. Edited by Ronald Wek

Cerebral palsy (CP) is a pediatric onset disorder with poorly understood molecular causes and progression, making early diagnosis difficult. Circular RNAs are regulatory RNAs that show promise as biomarkers in various diseases but the role of circular RNAs in CP is beginning to be understood. This study identified the role of circNFIX in regulating the expression of myocyte-specific enhancer factor 2C (MEF2C), an important transcription factor for sarcomere development. We found that circNFIX is downregulated in the muscle cells of individuals with CP, and its localization shifts toward the nucleus as visualized using single-molecule resolution imaging. The decreased expression of circNFIX, MEF2C, and MEF2C targets persisted throughout myoblasts to myotubes differentiation, and in the skeletal muscle tissue. Bioinformatic and experimental validation confirmed that circNFIX acts as a sponge for miR373-3p, a microRNA that represses MEF2C translation. In normal muscle, circNFIX derepresses MEF2C translation by sponging miR373-3p, allowing for normal sarcomere generation. In CP, reduced circNFIX expression results in loss of miRNA sponging, leading to lower MEF2C expression and downregulation of sarcomere genes, potentially causing shortened and dysfunctional muscle fibers. Knockdown (KD) of circNFIX reduced myogenic capacity of myoblasts to fuse and form myotubes similar to CP cells evident from the lower fusion index in CP and KD as compared to control myotubes. This is the first study reporting reduction of MEF2C in CP and single-molecule resolution imaging of circNFIX's subcellular distribution and its role in CP, suggesting circNFIX as a potential therapeutic target and biomarker for early CP diagnosis.

Cerebral palsy (CP) is a group of static encephalopathies associated with difficulties with movement, posture, and activity (1). It is the most common and severe, pediatric-onset motor disability with an estimated prevalence of 1 in 345 children (https://www.cdc.gov/cerebral-palsy/). Spastic-type CP accounts for more than 75% of the cases and involves muscle hypertonia, contracture, weakness, and musculoskeletal deformities that often worsen over time (2–5). These muscular conditions result in significant debilitation and often require surgical correction (5, 6). Due to a lack of well-defined genetic markers, diagnosis of CP is often delayed until children miss milestones, leading to a loss of critical time where supportive therapies could be implemented to prevent impairment progression and improve outcomes. Skeletal muscle-resident stem cells (satellite cells; SCs) play important roles in many of the effects seen in CP, and studies indicate that children with CP have unexplained reductions in their SC populations (7–10). Furthermore, the average sarcomere length is almost twice that of typically developing children; this sarcomere length difference likely contributes to the poor muscle force-generating capacity and weakness observed in children with CP (7, 11). Unfortunately, the molecular and cellular mechanisms leading to decreased SC content, increased sarcomere lengths, and other musculoskeletal pathologies in CP are largely unknown, and studies of muscle and SC involvement in CP are needed to help reduce progressive impairment, decrease the need for invasive surgery, and improve motor function and life quality of individuals with CP.

Muscle-resident SCs are critical for muscle growth, repair, and function, and SCs play important roles in many of the musculoskeletal attributes of CP. For example, neuromuscular junctions exhibit disrupted microanatomy, and SCs are known to contribute postsynaptic myonuclei with defined gene expression programs to neuromuscular junctions (NMJs) such that a lack of SCs contributes to NMJ degeneration (12–14). Interestingly, isolated SCs from CP muscle appear to be functionally and phenotypically different from controls in culture, and recent studies show that cells isolated from individuals with CP retain intrinsic differences that carry through daughter cells in culture (15, 16). The mechanisms accounting for the genesis and retention of SC differences in CP are not known. However, regulatory RNAs, which have been shown to play physiologically important roles in other musculoskeletal disorders, are promising potential candidates, and their role in CP is just beginning to be appreciated (17–19).

Circular RNAs (circRNAs) are the most recently recognized, and the least studied, members of the functional regulatory RNA family (20). These noncoding RNAs (ncRNAs) were discovered >30 years ago when transcripts that

* For correspondence: Mona Batish, batish@udel.edu.

displayed out-of-order exons were observed (*i.e.*, downstream exons appeared prior to their upstream neighbors) (21, 22). Circularization of linear transcripts occurs between the 3′ splicing donor and the 5′splicing acceptor site through a noncanonical splicing event called back splicing (23, 24). It is estimated that on average 1 to 2% of all mRNA species generate circRNAs (25). The circRNAs lack a poly-A tail and are not usually translated (26), although there have been some reports on circRNA-encoded proteins (27, 28). The most common functions attributed to circRNAs are as follows: (i) sequestration of microRNAs (therefore often referred to as "microRNA sponges") (29), (ii) regulation of splicing and transcription (30) and (iii) regulation of their parent gene expression (31, 32). These are highly enriched in the brain and involved in various neurological disorders (33). The circRNAs have been shown to play a role in muscle development using animal models, but their role in myogenesis and NMJ disruption with respect to CP has not yet been explored (34, 35).

One of the recently characterized circRNAs for its role in myogenesis in mouse models is a super enhancer-associated circRNA produced from exon 2 of nuclear factor IX (*NFIX*) gene. This circRNA is produced by back splicing of exon 2 of the *NFIX* gene and yields a spliced product of 532 bases (hsa-circ-0005660). It is conserved across species and is abundant in heart muscles and participates in the development of the brain, heart, and other organs (36, 37). Its overexpression is shown to inhibit cardiomyocyte proliferation (38).

Knockdown of circNFIX is reported to lead to cell cycle arrest, inhibition of glycolysis, migration and invasion, and promotion of apoptosis in glioma cells, hepatocellular carcinoma, and non–small cell lung cancer cells (39–42). The circNFIX was shown to be a molecular marker of glioma in humans (42, 43). Most recently, our collaborators have shown that circNFIX might regulate the expression of myocyte-specific enhancer factor 2C (MEF2C) by sponging miR-204-3p in mouse skeletal muscle cells (37). MEF2C is a transcription factor that controls muscle development, interacts with a variety of proteins, including MECP2 and CDKL5, and mediates later differentiation stages in myogenesis (44, 45). Several reports have shown that MEF2C regulates the expression of sarcomere genes and thus downregulation of MEF2C could disrupt sarcomere organization and impact muscle development leading to muscle pathologies reported in CP (45–47). Thus, we asked if circNFIX is regulating MEF2C expression in myoblasts and myotubes derived from human skeletal muscle and if dysregulation of circNFIX levels in cells derived from individuals with CP could help us to explain alterations in SCs and abnormalities in sarcomere lengths and functions in CP.

Results

Expression profile of circNFIX in human satellite cells-derived myoblast

Human satellite cells-derived myoblasts (SC-MBs) were isolated from skeletal muscle biopsies of nine control (CN) and nine cerebral palsy (CP) patients of both sexes and ages ranging from 10 to 19 years old (Table S1). This was done under an Institutional Review Board (IRB)-approved protocol (protocol number 687629) at the Nemours Children's Hospital, Wilmington, DE, USA. The SC-MBs were isolated first using immunomagnetic separation to enrich neuronal cell adhesion molecule and chemokine receptor type 4 positive cells as outlined in Figure 1*A*. The validation of SC-MBs was done based on the expression of SC signature markers, PAX7 and MYF5, using immunofluorescence. Both CN and CP SC-MBs showed a uniform expression of both markers, as demonstrated in Figure 1*B*.

To evaluate the expression levels of circNFIX in the SC-MBs derived from CN and CP individuals, we used a two step quantitative reverse transcriptase PCR (qRT-PCR) to amplify circNFIX RNA from these cells. Toward this, a set of divergent primers was designed to target the back splice junction of the circNFIX so that the linear transcript does not get amplified. The identity of circNFIX was confirmed by Sanger sequencing of the PCR product (Fig. 2*A*). As a control, we included conventional convergent primers for linear NFIX and MEF2C. Interestingly, upon averaging the qRT-PCR data from all 9 CP derived SC-MBs, a reduction of 18% and 23% in the expression level of circNFIX and MEF2C was seen respectively when normalized to their levels in all 9 CN derived SC-MB samples (Fig. 2*B*). To validate that circRNA is free of any linear RNA, the total RNA of SC-MBs was treated with RNase R, an exonuclease that degrades the linear RNA but not circRNA forms due to the lack of open ends (48). We confirmed that circNFIX is resistant to RNase R and did not get cleaved after treatment, while the MEF2C and GAPDH mRNA levels decreased significantly by 97% in the RNAase R-treated samples compared to the untreated samples (Fig. 2*C*).

Next, we asked if this reduction in expression level of circNFIX and MEF2C has a functional relevance in the SC-MBs. For this, we created a stable knockdown of circNFIX using shRNA specific to the unique back splice junction of circNFIX in the SC-MBs derived from control tissue samples and termed it as CN circNFIX KD (referred to as KD here after for simplicity). We also created a negative control using the scrambled sequence of the shRNA and termed it scramble (SCR). As expected, the level of circNFIX reduced only in KD while it did not change in SCR (Fig. 3*A*). To confirm the specificity of shRNA knockdown, we also checked the levels of linear NFIX and MEF2C in the KD and SCR cells. We did not see any change in SCR for either of the three candidates while the linear NFIX expression showed a nonsignificant increase. Interestingly, MEF2C levels were reduced significantly in KD which is consistent with the loss of MEF2C in CP-derived SC-MBs, indicating that circNFIX might be helping to maintain MEF2C levels in the SC-MB cells. To further confirm the effect of circNFIX on MEF2C protein levels, we conducted immunofluorescence assays for MEF2C protein levels, which revealed a significant reduction in MEF2C levels in both CP and KD SC-MBs as compared to CN (as shown in Fig. 3*B*). Western blot analysis showed no detectable levels of MEF2C protein in CP and circNFIX KD cells while it was seen in CN SC-MBs (Fig. S4*A*).

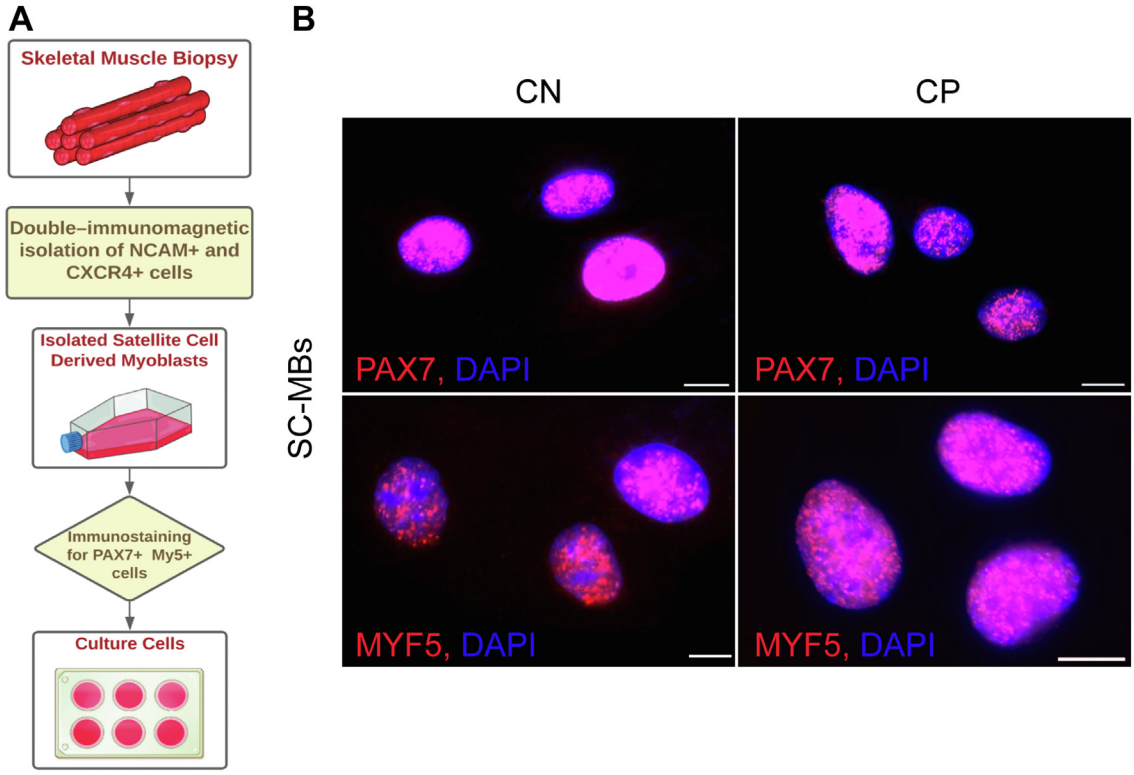

Figure 1. Verification of isolated satellite cells. *A*, graphical representation of workflow of isolating satellite cells derived myoblasts from muscle biopsies. *B*, representative immunofluorescence images of SC-MBs isolated from control (CN) and cerebral palsy (CP) stained with anti-PAX7 and anti-MYF5 antibodies. PAX7 and MYF5 signals are pseudo colored *red* and merged with DAPI staining shown as *blue*. The scale bar represents 5 μm. SC-MB, satellite cell-derived myoblast; DAPI, 4′,6-diamidino-2-phenylindole.

The reduction in RNA and protein levels of MEF2C upon knockdown of circNFIX implied that circNFIX is involved in regulating MEF2C levels in SC cells. One of the direct ways to evaluate this effect is to identify if circNFIX KD affects the amount of MEF2C RNA engaged with polysomes which is indicative of actively translated RNAs. Toward this, we performed polysome profiling using a size-exclusion column as described in the methods (49) on cell lysates from CN, CP, and KD SC-MBs cells. The UV chromatograms of size-exclusion chromatography (SEC) showed a clean separation of polysomes and nonpolysome fractions from all samples (Fig. 4*A*). The first peak with the shortest retention time had a small height and was collected and labeled as the polysome bound (PB) fraction. We pooled all the other non-polysome fractions (containing ribosomal subunits including 80S, 60S, and 40S) and labeled it as non-PB fraction. Subsequently, we isolated total RNA from both PB and non-PB bound fractions and performed qRT-PCR to compare the level of MEF2C mRNA between these two fractions. Our findings revealed that MEF2C RNA is highly enriched in the non-polysome fraction

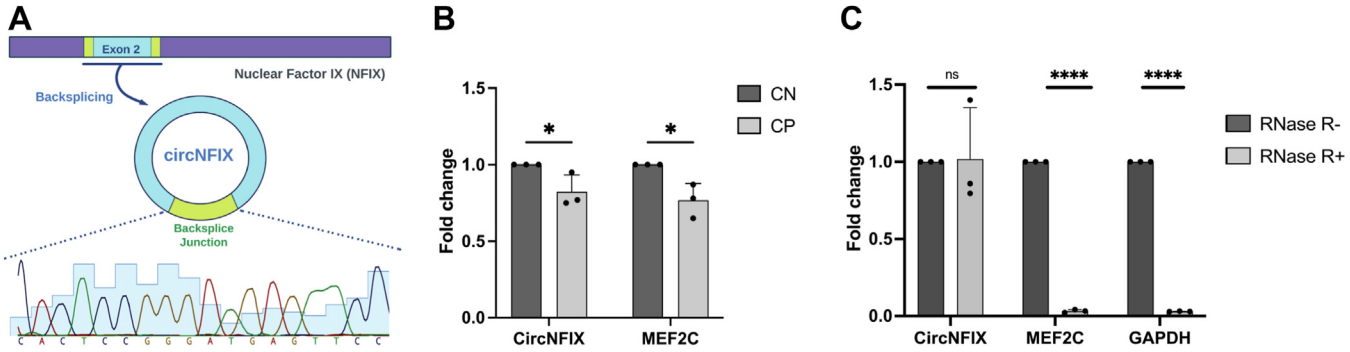

Figure 2. Validating expression of circNFIX and MEF2C in SC-MBs. *A*, graphical representation of circNFIX and validation of the back splice junction of circNFIX by Sanger sequencing of the PCR product obtained using divergent primers using RNA isolated from SC-MBs. *B*, average fold change in expression levels of circNFIX and MEF2C RNA between nine control (CN) and nine CP derived SC-MBs by qRT-PCR. *C*, relative expression levels of circNFIX, MEF2C, and GAPDH RNA represented as fold changes upon treatment with RNase R (RNase R+) compared to untreated samples (RNase R-). Error bars indicate standard deviation. Significance (* = $p < 0.05$, **** = $p < 0.0001$, ns = not significant) was established using unpaired, two-tailed Student's *t* test. All experiments were performed in triplicate. CP, cerebral palsy; MEF2C, myocyte-specific enhancer factor 2C; NFIX, nuclear factor IX; qRT-PCR, quantitative reverse transcriptase PCR; SC-MB, satellite cell-derived myoblast.

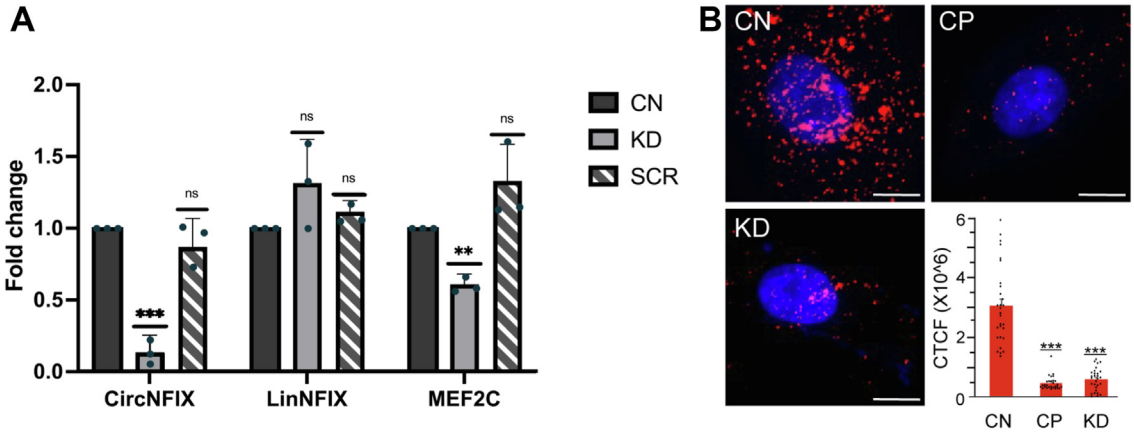

Figure 3. Effect of circNFIX knockdown on MEF2C. *A*, fold change in expression levels of circNFIX and MEF2C RNA between control (CN), CN circNFIX KD (KD), and CN scramble (SCR) SC-MBs by qRT-PCR. *B*, representative images and quantification of MEF2C protein levels (corrected total cell fluorescence–CTCF) measured by immunofluorescence confirming downregulation of MEF2C protein in CP and KD. *Red dots* depicting MEF2C protein are merged with DAPI (*blue*). Error bars indicate standard deviation. Significance (* = $p < 0.05$, ** = $p < 0.01$, *** = $p < 0.001$, ns = not significant) was established using unpaired, two-tailed Student's *t* test. All experiments were performed in triplicate. The scale bar represents 5 μm. CP, cerebral palsy; DAPI, 4′,6-diamidino-2-phenylindole; MEF2C, myocyte-specific enhancer factor 2C; NFIX, nuclear factor IX; qRT-PCR, quantitative reverse transcriptase PCR; SC-MB, satellite cell-derived myoblast.

in both CP and KD, when compared to the respective CN SC-MB (Fig. 4*B*). These results strongly support the notion that circNFIX is involved in regulating the translation of MEF2C protein.

Determination of intracellular localization of circNFIX

Notably, conventional methods of analyzing circRNAs, and ncRNAs generally do not provide cellular localization; however, the function of ncRNAs is largely determined by where they are located within the cell (50). The standard method for imaging circRNAs uses a single probe specific to the unique back splice junction, formed by the joining of exon ends (51). However, this method does not provide single-molecule resolution without substantial signal amplification, which often leads to high background and nonspecific signals causing misleading results about colocalization and molecular interactions (52). Recently, we have developed a new method to specifically identify and localize circRNAs *in situ*. Following our previously developed method of "fusion-FISH" for the sensitive detection of linear fusion transcripts (53), "circFISH" has been developed for the detection of circRNAs simultaneously with their linear counterparts (54). Here, two sets of probes are designed with each set containing ∼ 40 oligonucleotides, each 20 nt in length and labeled with the same single fluorophore at the 3′end. The first probe set called probe circular (PC) is designed to bind exon 2 found in both

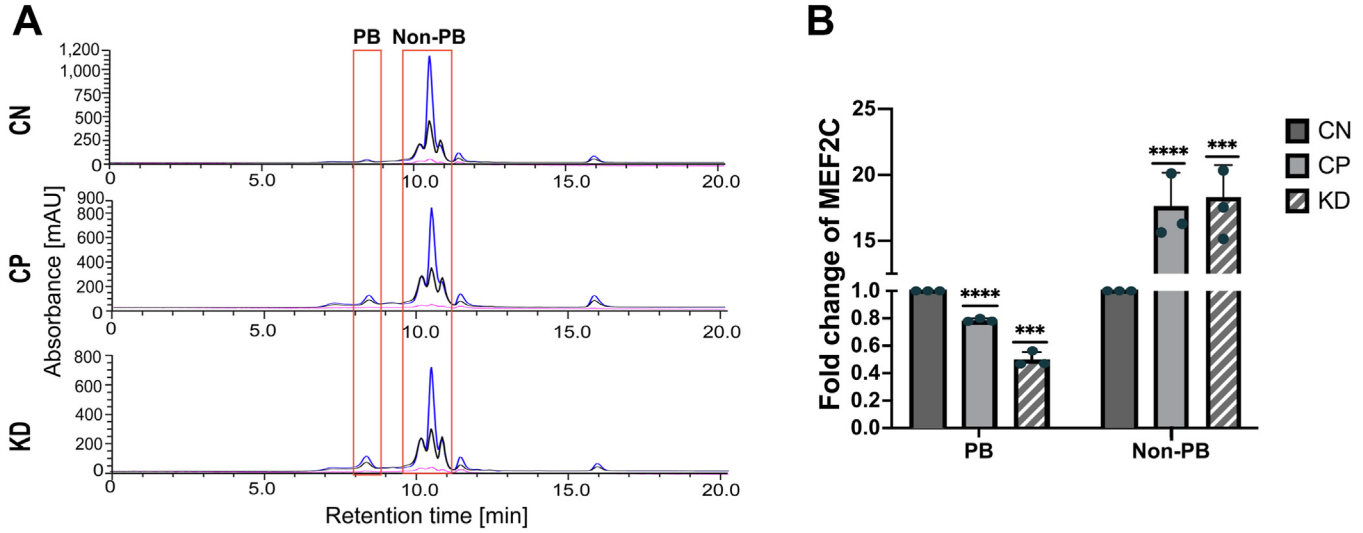

Figure 4. Polysome fractionation of MEF2C mRNA distri. *A*, the UV chromatograms of SEC from CN, CP, and CN circNFIX KD. Polysome bound (PB) represents mRNA bound to polysomes, while non-polysome bound (non-PB) represents mRNAs bound to ribosomal subunits, including 80S, 60S, and 40S. The *x*-axis indicates the retention time, and the *y*-axis shows the UV absorbance at 215 nm (*pink line*), 260 nm (*blue line*), and 280 nm (*black line*). *B*, the fractions were analyzed by qRT-PCR. The expression of MEF2C mRNA was normalized with GAPDH to compare its expression in CP and KD samples in polysomes (PB) and subunits (non-PB). Error bars indicate standard deviation. Significance (*** = $p < 0.001$, **** = $p < 0.0001$) was established using unpaired, two-tailed Student's *t* test. All experiments were performed in triplicate. CN, control; CP, cerebral palsy; MEF2C, myocyte-specific enhancer factor 2C; NFIX, nuclear factor IX; qRT-PCR, quantitative reverse transcriptase PCR; SEC, size-exclusion chromatography.

circNFIX and linear NFIX, and the second probe set called probe linear (PL) is designed to bind exon 11 of the NFIX mRNA which is only found in linear NFIX (Fig. 5*A*). Thus, circNFIX will show signal from just the PC probe while linear NFIX will have a colocalized signal from both PC and PL probe sets. Using circFISH, SC-MBs showed distinct spots for linear NFIX and circNFIX. Linear NFIX was almost exclusively found in the cytoplasm, while circNFIX was distributed 88% in the cytoplasm and 12% in the nucleus. Interestingly, in SC-MBs from CP, the nuclear fraction increased to 17% and the cytoplasmic fraction became 83%. Although small, there was a statistically significant increase in the nuclear localization of circNFIX in SC-MB derived from CP compared to CN, while no such change was observed for linear NFIX RNA. This indicates that there is a change in both the level and distribution of circNFIX in CP implying that circNFIX might be translocating to the nucleus upon the onset of CP (Fig. 5, *B*, bottom panel and *C*). Since circFISH is single-molecule resolution, we quantified the spots for linear and circNFIX and found that circNFIX is highly expressed with an average copy number of 60 copies/cell in CN and 30 copies/cell in CP-derived SC-MB (Fig. 5*D*). A standard control to validate circRNAs is their ability to withstand RNase R treatment (55). Thus, we performed RNase R treatment *in situ*, which caused a significant loss of only linear NFIX and corroborated the authenticity of circFISH imaging (Figs. 5, *B*, second panel, and *D* and S1). Moreover, performing circFISH in KD SC-MBs showed a reduction in circNFIX levels further supporting knockdown efficiency. The qRT-PCR data also corroborated these results, demonstrating the sensitivity and specificity of circFISH (Fig. 5, *B* third panel, and *D*).

Determination of the role of circNFIX in SC-MBs

The most well-studied functional mechanism of circRNAs is their ability to sponge miRNAs. This has indeed been observed for circNFIX in a mouse model where circNFIX was postulated to regulate MEF2C expression levels by sponging miR-204 (37). Our data so far have supported the regulation of MEF2C by circNFIX in human cells, but we were missing the miRNA involved (if any) in this circRNA-miRNA-mRNA axis. Since most miRNAs function by interacting with the 3′UTR of target RNA, we analyzed the 3′UTR of MEF2C. It is rather long and harbors potential binding sites for thousands of miRNAs. To narrow down the miRNAs for future exploration, we split the 3′UTR of MEF2C into three nonoverlapping fragments and cloned each of these fragments at the end of *Renilla* luciferase coding region in the dual luciferase plasmids containing *Renilla* (RL) and firefly (FL) luciferase genes (56) (Fig. 6*A*). We transfected CN, CP, KD, and SCR SC-MBs with this construct and performed the luciferase assay. The results showed that there was a significant decrease in luciferase activity 24 h post

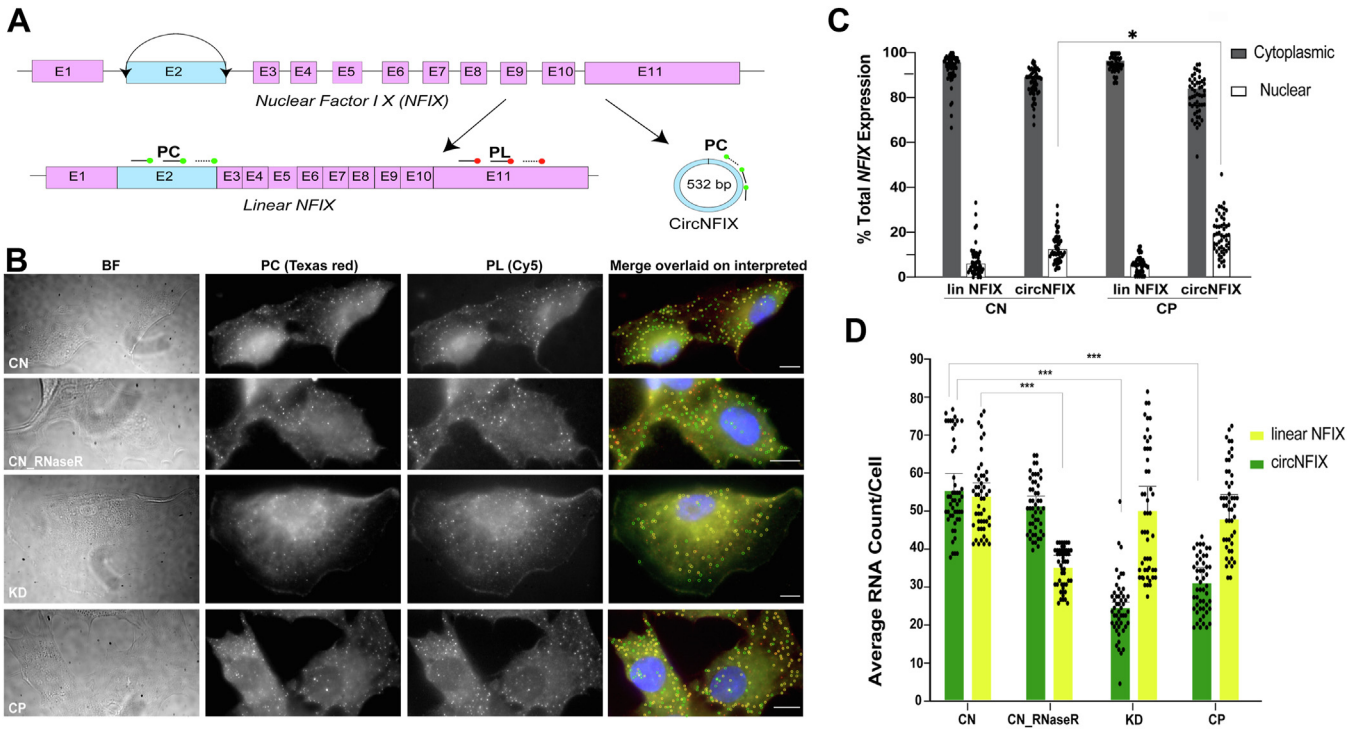

Figure 5. Cellular localization of circNFIX and linear NFIX at single molecule resolution. *A*, schematic showing biogenesis of the linear and circular NFIX transcripts from the *NFIX* gene as well as the binding sites of PC (probes binding exon 2, found in both circNFIX and linear NFIX) and PL (probes binding exon 11, only found in linear NFIX) probes. *B*, representative images of SC-MBs from control (CN), control treated with RNase R, KD, and CP. *Left* most panels are bright field images of cells, *middle* panels are merged z stacks of raw images in Texas red (PC) and Cy5 (PL) channels, right most panels show merge of two channels (*Texas red* pseudo colored as *green*, Cy5 pseudo colored as *red* over DAPI. *C*, nuclear and cytoplasmic distribution of linear and circNFIX in CN- and CP-derived SCMBs. *D*, quantification of circFISH images from CN, CN treated with RNase R, CN circNFIX knockdown, and CP-derived SC-MBs. At least 100 cells were counted for each set, each experiment was performed in triplicate. Error bars indicate 95% CI. Significance (* = $p < 0.05$, *** = $p < 0.005$) was established using unpaired, two-tailed Student's *t* test. Scale bar is 5 μm. CI, confidence interval; DAPI, 4′,6-diamidino-2-phenylindole; NFIX, nuclear factor IX; SC-MB, satellite cell-derived myoblast.

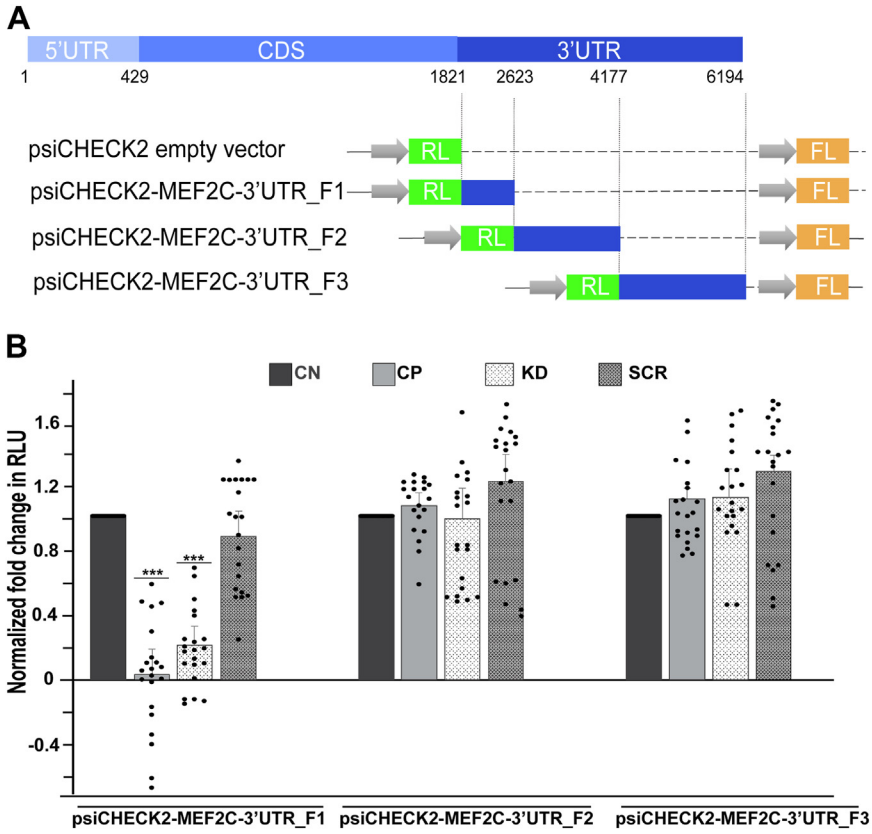

Figure 6. Identification of miRNA binding site in the 3′UTR of MEF2C. *A*, schematic of MEF2C 3′ UTR regions used in the luciferase assay. *B*, the results of the luciferase assay after transfecting SC-MBs from control (CN), CP, CN cNFIX KD, and CN SCR with psiCHECK2 dual-luciferase vectors expressing different fragments of 3′UTRs of MEF2C in frame with *Renilla* luciferase. Cells were lysed 24 h post transfection, and the expression of *Renilla (RL)* and firefly (*FL*) was measured in relative light units (RLU) for three different fragments (F1, F2, and F3) of the MEF2C 3′ UTR, empty vector, and mock transfection sample. We calculated the ratio of renilla luciferase/firefly luciferase (RL/FL) for all the samples and normalized the RL/FL of F1, F2, and F3 samples to RL/FL of mock transfection, and then to RL/FL of empty plasmid by subtraction. The normalized RL/FL of CP, CN circNFIX KD, and CN SCR was compared to the respective normalized RL/FL of CN SC-MBs. All experiments were done in triplicate. Error bars indicate 95% CI. Significance (*** = $p < 0.001$) was established using unpaired, two-tailed Student 's *t* test. CI, confidence interval; CN, control; CP, cerebral palsy; MEF2C, myocyte-specific enhancer factor 2C; NFIX, nuclear factor IX; SC-MB, satellite cell-derived myoblast.

transfection in CP and CN circNFIX KD cells when compared to CN SC-MBs. This decrease was observed only with the MEF2C UTR fragment 1, which suggests that circNFIX is likely sponging the miRNA(s) that interact through fragment 1 of MEF2C 3′ UTR. Moreover, the luciferase activity did not show any changes in the CN SCR when compared to CN SC-MBs, denoting that the effect is specific to the CP and KD cells (Fig. 6*B*).

Determination of the circRNA-miRNA-mRNA regulatory interaction

The above experiment helped us to narrow down to a smaller list of miRNAs. Another requirement for the candidate miRNAs is that circNFIX should have a binding site for this miRNA. Toward this, we decided to predict all the miRNA targets for circNFIX and MEF2C 3′UTR fragment 1 using three different bioinformatics tools including TargetScan, miRanda, and miRDB (57–60). After identifying binding sites for over 200 miRNAs in both circNFIX and MEF2C (57, 61), we analyzed the miRNAs targeting both *MEF2C* 3′UTR fragment 1 and circNFIX, revealing 23 overlapping miRNAs (Fig. 7*A*). We analyzed these 23 miRNAs by comparing them to the expression profile of miRNAs in human skeletal muscle cells and the miRTarBase v8 database (62) (Fig. 7*B*). This comparison narrowed down the list to 19 miRNA targets, which were further analyzed for their validated targets and muscle-specific expression reported by miRNATissueAtlas2 (62, 63). Finally, we identified four muscle-specific functional miRNAs that are predicted to target *MEF2C* 3′UTR fragment 1 by at least two prediction tools (Fig. 7*C*). Using qRT-PCR, we found that miR-373-3p was consistently expressed in the SC-MBs from all nine control and nine CP samples. We also found that miR-373-3p levels were slightly higher in SC-MBs from CP samples as compared to the controls but did not show any significant reduction in KD (Fig. 7*D*). This is expected as it is known that circRNAs do not affect the level of miRNA expression but rather suppress their function by acting as a competing endogenous RNA. Therefore, we should not expect to see any significant change in target miRNA levels upon circRNA KD.

To fully underscore the relevance of competitive binding of circNFIX to miR373-3p, the stoichiometry of their expression should be evaluated. Toward this, we used digital PCR to determine the copy number of circNFIX and miR-373-3p. Our

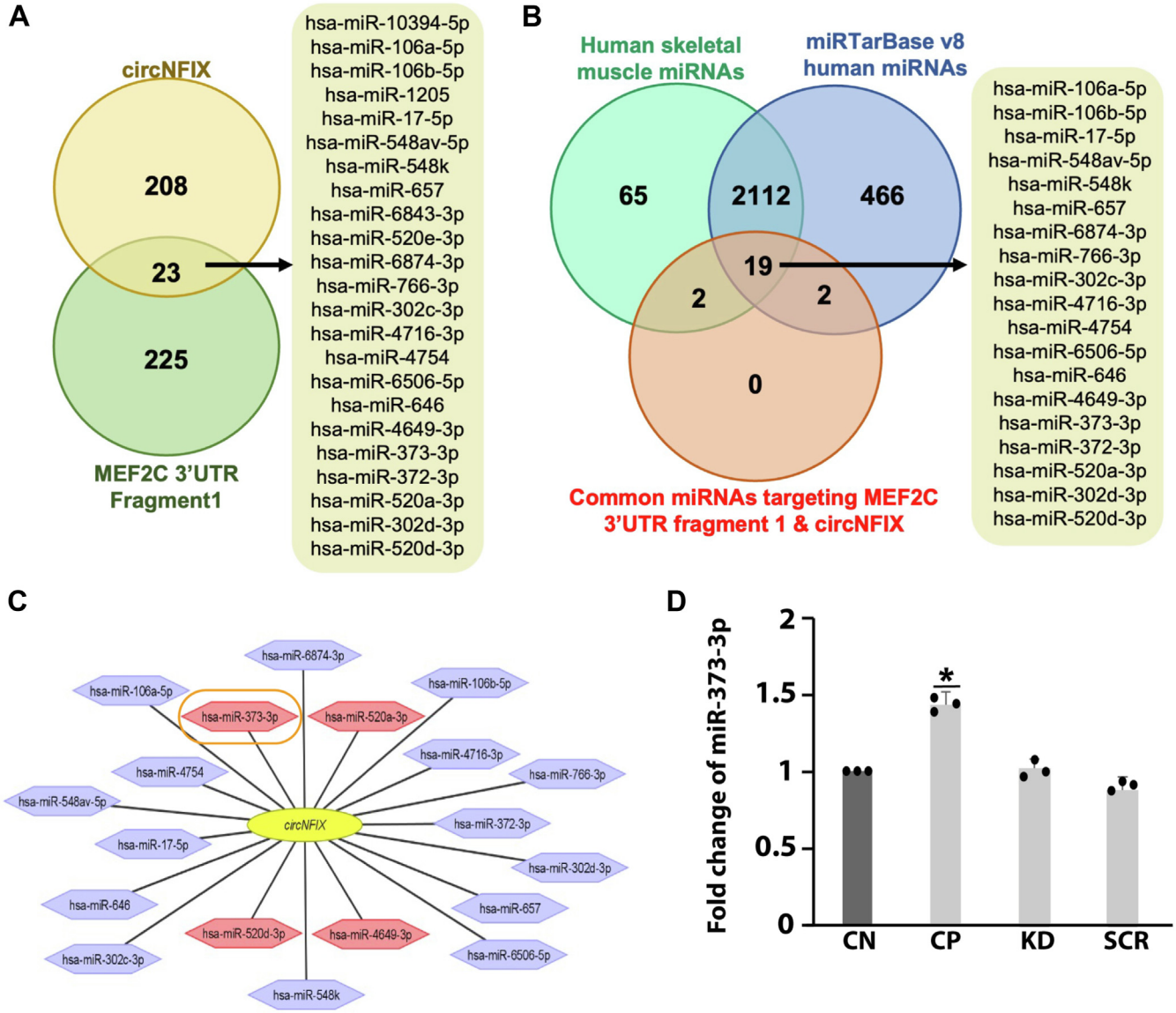

Figure 7. Bioinformatic analysis to identify miRNAs interacting with circNFIX and MEF2C. *A*, common human miRNAs predicted to interact with circNFIX and MEF2C 3′UTR fragment 1. *B*, common muscle specific miRNAs reported in miRTarBase and associated with both circNFIX and MEF2C 3′UTR fragment 1. *C*, functional miRNAs associated with circNFIX-MEF2C mediated regulation in human skeletal muscle. *Red color* indicates muscle miRNAs and predicted to bind to MEF2C 3′ UTR fragment 1 by two different miRNA analysis algorithms. *D*, expression levels of miR-373-3p in SC-MBs from CN, CP, KD, and SCR measured by qRT-PCR. Each experiment was performed in triplicate. Error bars indicate standard deviation. Significance (* = $p < 0.05$) was established using unpaired, two-tailed Student's *t* test. CN, control; CP, cerebral palsy; MEF2C, myocyte-specific enhancer factor 2C; NFIX, nuclear factor IX; qRT-PCR, quantitative reverse transcriptase PCR; SC-MB, satellite cell-derived myoblast.

findings revealed that circNFIX is highly expressed with an average copy number of 64 copies/cell, while miR-373-3p is expressed at lower levels, with an average of 43 copies/cell in CN SC-MBs. These results are consistent with RNA counts obtained through circFISH imaging as well as the qRT-PCR data. This provides solid support for our hypothesis that due to high expression levels, sponging of miR373-3p by circNFIX will render the miRNA unavailable to bind to MEF2C, thereby blocking its translation. Furthermore, we combined circFISH and double-fluorescein amidites-labeled miRCURY LNA miRNA detection probes to directly visualize the interaction between circNFIX and miR373-3p. Although the signals were not as clean as circFISH alone due to multiple extended hybridization steps and treatments, we were indeed able to observe several spots where miR-373-3p and circNFIX signals were overlapping, indicating the interaction between these two molecules is real and biologically relevant (Fig. S2).

Functional validation of the circRNA regulatory axis in SC-MBs

To functionally validate if circNFIX is indeed acting *via* miR-373-3p to exert its regulatory role on the expression of MEF2C, we transfected the CN-derived SC-MBs with a mimic of miR-373-3p along with the dual luciferase construct containing the fragment 1 of MEF2C 3′UTR. The introduction of the miRNA mimic should increase the level of miR-373-3p in

the cell, enabling binding to the target MEF2C mRNA, and thus leading to a reduction in luciferase expression. As seen in Figure 8*A*, a decrease in luciferase activity was noticed in a dose-dependent manner. This was measured *via* a dual luciferase assay 24 h after transfection of the reporter and different concentrations of miR-373-3p mimic. We found that 20 nM of mimic reduced the signal by almost 60 percent, indicating a significant functional effect of miR373-3p in regulating luciferase protein expression.

To further validate this finding, we identified the exact binding site of miRNA-373-3p in the MEF2C 3′UTR fragment 1 and mutated it in the dual luciferase construct using site-directed mutagenesis such that miR373-3p could no longer bind to this mutated construct (Fig. 8*B*). Transfection of CN SC-MBs with 10 nM mimic and the mutated fragment 1 construct did not significantly change luciferase activity compared to CN cells that were not transfected with mimic. On the other hand, the luciferase activity was significantly reduced when 10 nM miRNA-373-3p mimic was added along with the WT construct containing fragment 1 compared to CN SC-MBs cells that were not transfected with mimic (Fig. 8*C*). Furthermore, a negative control miRNA was used to confirm the specificity of miR-373-3p on the luciferase activity. Transfecting CN SC-MBs with 10 nM of mirVana miRNA Mimic Negative Control #1 (NC) mimic did not result in a significant change in the luciferase activity when normalized to the no treatment control (NT) where in no mimic was added (Fig. 8*D*). The mirVana miRNA Mimic Negative Control from Thermo Fisher Scientific is a randomized miRNA molecule that has been extensively tested to have no identifiable effects on known miRNA function in human cell lines and tissues. The luciferase data further validated the functional effects of circNFIX:miR373-3p:MEF2C regulation.

Expression profile of circNFIX and MEF2C in human SC-derived myotubes and skeletal muscle tissue

Multiple lines of evidence have helped us to understand the regulation of MEF2C by circNFIX, but it is imperative to know if this effect is limited to the stage of myoblast proliferation or if it persists through the development of these SC-MBs into myotubes and reflects in the muscle tissue. Therefore, the SC-MBs from nine control and nine CP patients were differentiated for 72 h in differentiation medium to induce myotube

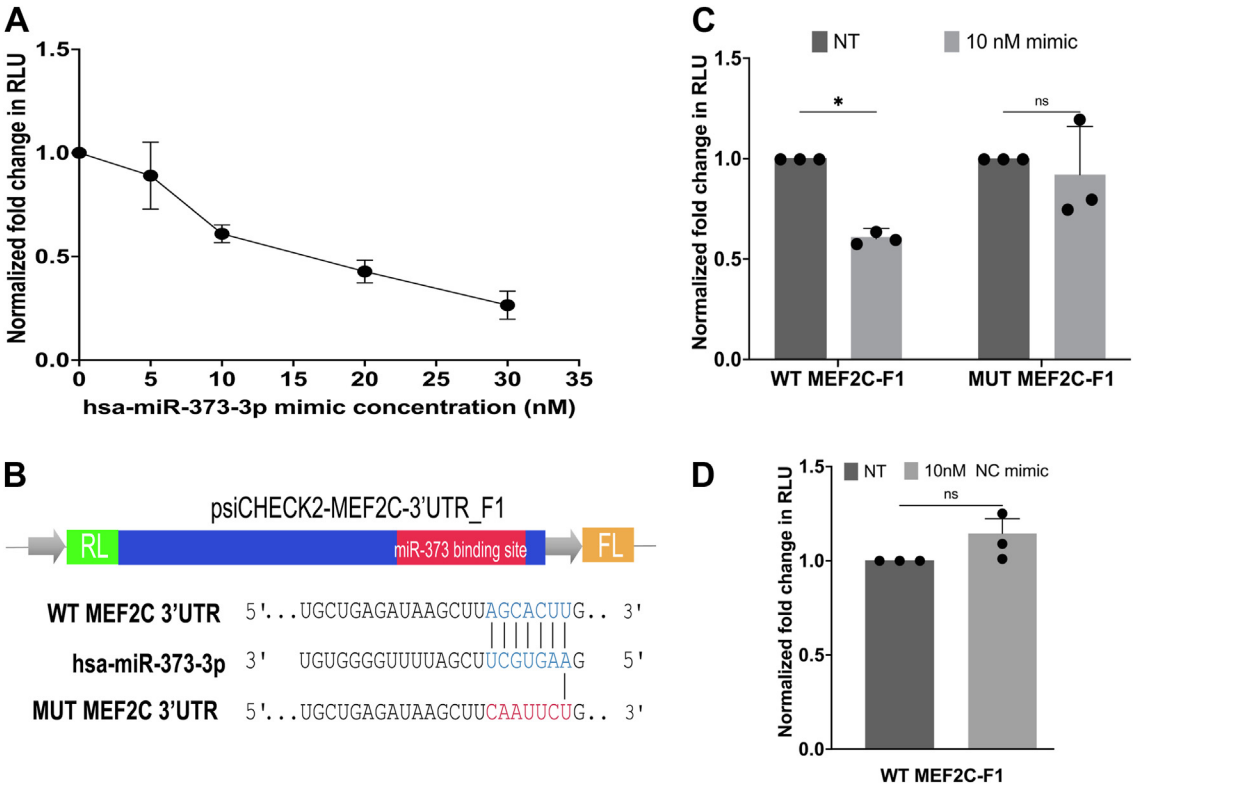

Figure 8. Luciferase assay to confirm specific interaction between miR-373-3p and MEF2C. *A*, the normalized fold change in Relative Light Unit (RLU) after 24-h post transfection with increasing concentrations of hsa-miR-373-3p mimic to SC-MBs from control (CN) samples. The relative expression of *Renilla* normalized to firefly did not change upon increasing concentrations of mimic (Fig. S3). *B*, pairwise alignment between miR-373-3p and the WT and mutated dual luciferase construct expressing fragment 1 of MEF2C 3′UTR. *C*, luciferase assay using SC-MBs from control (CN) transfected with psiCHECK2 dual-luciferase vectors expressing either WT or mutated fragment 1. Each assay was performed in the presence of 10 nM of hsa-miR-373-3P mimic or NT (no treatment control) indicating absence of the mimic was used to normalize the readings. *D*, normalized fold change in RLU after transfecting control SC-MBs with WT dual luciferase construct expressing fragment 1 of MEF2C 3′UTR along with 10 nM of mirVana miRNA Mimic Negative Control #1 (NC) mimic or No treatment (NT) which include no mimic. Cells were lysed 24 h post transfection and the ratio of *Renilla* to firefly RLU was normalized to empty psicHECK2 plasmid. Error bars indicate standard deviation. Significance (* = $p < 0.05$, ns = no significant) was established using unpaired, two-tailed Student's *t* test. All the experiments were repeated in triplicate and on cells obtained from multiple samples. MEF2C, myocyte-specific enhancer factor 2C; SC-MB, satellite cell-derived myoblast.

(SC-MT) formation (Table S1). The cells showed typical morphology of multinucleated elongated cells upon differentiation. RNA was isolated from SC-MTs derived from both the CN and CP samples and qRT-PCR was performed to check the expression of circNFIX and MEF2C. Averaging all the nine CN and nine CP samples found that both targets were significantly downregulated in CP derived SC-MTs as compared to CN SC-MTs. The circNFIX was reduced by 37% while MEF2C RNA was reduced by 51%. Similarly, the expression of circNFIX and MEF2C was significantly downregulated in the circNFIX KD SC-MTs when compared to the CN myotubes (Fig. 9*A*). Comparably, MEF2C protein expression (Fig. 9*B*) was lower in SC-MTs derived from CP and KD as compared to CN samples. Western blot analysis and the quantification of the percentage of MEF2C positive nuclei also revealed downregulation of MEF2C protein in CP and circNFIX KD cells compared to CN SC-MBs (Fig. S4, *B* and *C*). This demonstrated that the circNFIX-dependent downregulation of MEF2C persists throughout the differentiation process.

We wanted to further ask if the reduction in circNFIX would impact the expression of the downstream effector target genes of the MEF2C transcription factor. MEF2C is an important transcription factor that plays a crucial role in controlling the assembly of sarcomeres by regulating the expression of structural and sarcomeric genes such as myomesins, myozenins, myotilin, among others (45). We selected six major genes that are known to be controlled by MEF2C for proper sarcomere formation. Myomesins are proteins found in the M-band region of the sarcomere, and they play a crucial in maintaining sarcomere stability and enabling it to return to its original state after contraction (64). Myozenins are Z-line interacting proteins that link calcineurin with the sarcomere by acting as stress sensors (65). On the other hand, myotilin functions as an actin cross-linking protein and contributes to the structural integrity of the sarcomere (46). By qRT-PCR, we found that CP-derived SC-MTs have reduced expression of four of the six MEF2C targets (Fig. 10). CircNFIX KD myotubes also showed downregulation of MEF2C targets. These data provided evidence for our hypothesis that circNFIX-dependent reduction of MEF2C in SCs imparts its effect and leads to alteration in functional sarcomere formation in SC-MTs.

Our findings in SC-MTs indicated that the dysregulation of circNFIX persists throughout the differentiation process. All of these data originated from using isolated SCs in 2D culture which could have artifacts and might lose contextual

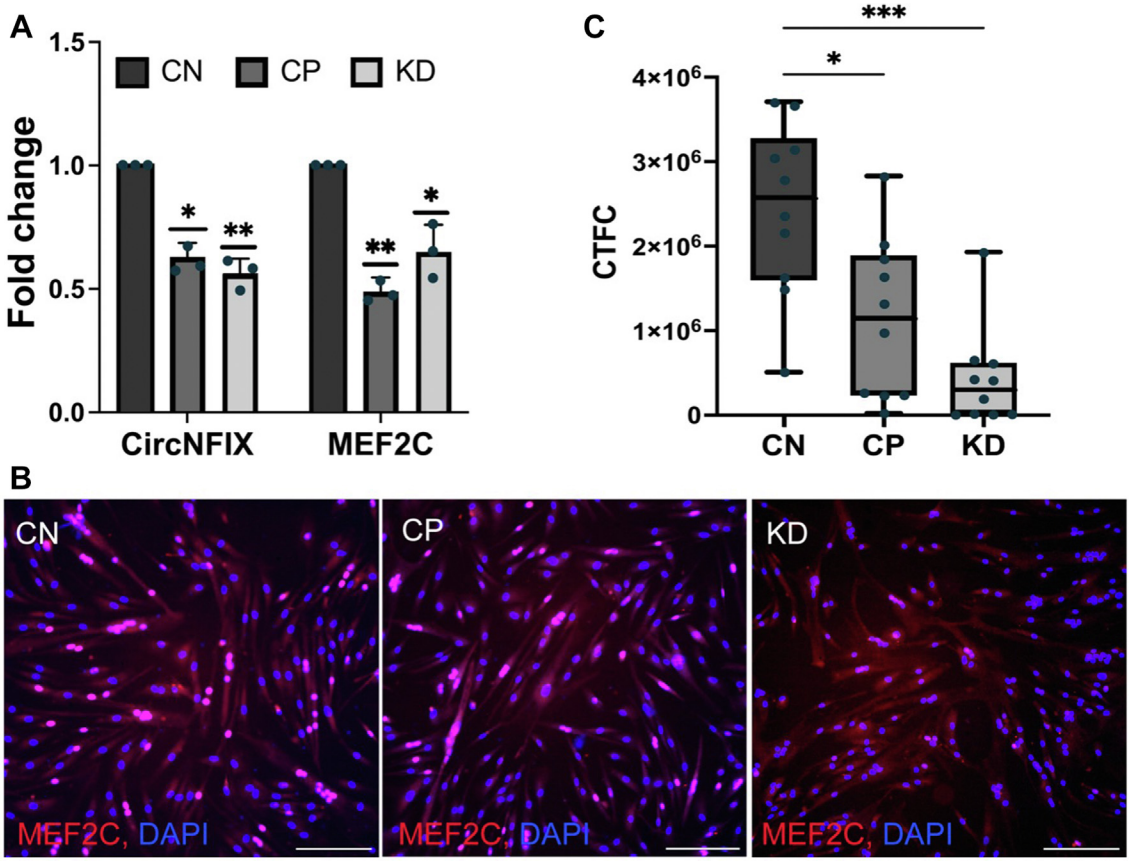

Figure 9. Effect of circNFIX reduction on MEF2C expression in myotubes derived from satellite cells. *A*, fold change in expression levels of circNFIX and MEF2C RNA between control (CN) and CP derived SC-MTs by qRT-PCR. *B*, representative images of MEF2C protein levels. *Red dots* depicting MEF2C protein are merged with DAPI (*blue*). *C*, corrected total cell fluorescence (CTCF) of MEF2C protein in CN and CP SC-MTs. Each experiment was performed in triplicate. Error bars indicate standard deviation. The *whiskers* of the box plot represent the minimum and maximum values. Significance (* = $p < 0.05$, ** = $p < 0.01$, ***= < 0.001) was established using unpaired, two-tailed Student's *t* test and Kruskal–Wallis test. The scale bar represents 10 μm. CP, cerebral palsy; DAPI, 4′,6-diamidino-2-phenylindole; MEF2C, myocyte-specific enhancer factor 2C; NFIX, nuclear factor IX; qRT-PCR, quantitative reverse transcriptase PCR; SC-MT, satellite cell-derived myotube.

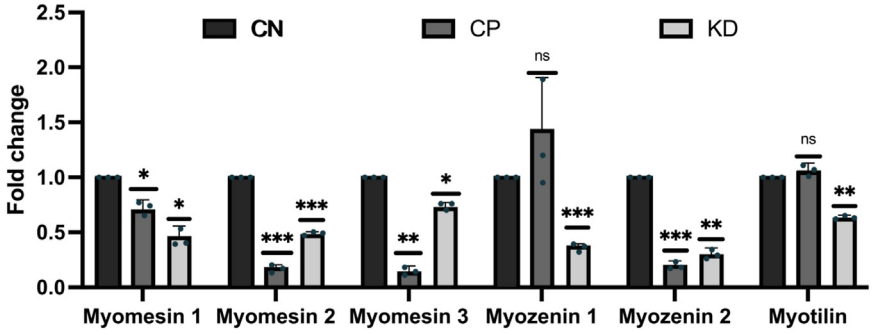

Figure 10. Expression levels of MEF2C downstream targets measured by qRT-PCR analysis in CN and CP, and circNFIX KD derived SC-MTs. The experiment was performed in triplicate. Error bars indicate standard deviation. Significance (* = $p < 0.05$; ** = $p < 0.01$; ** = $p < 0.001$; ns = not significant) was established using unpaired, two-tailed Student's *t* test. CN, control; CP, cerebral palsy; MEF2C, myocyte-specific enhancer factor 2C; NFIX, nuclear factor IX; qRT-PCR, quantitative reverse transcriptase PCR; SC-MT, satellite cell-derived myotube.

information of the tissue environment (66). To avoid this bias, we sought to investigate whether the low expression of circNFIX and MEF2C is seen in skeletal muscle tissue in CP patients. We isolated RNA directly from skeletal muscle biopsies of six CN and six CP patients of both sexes and ages ranging from 11 to 19 years old (Table S2). Notably, our results showed that circNFIX and MEF2C expression was lower in skeletal muscle tissue of individuals with CP compared to CN. The circNFIX was reduced by 29% while MEF2C was reduced by 19% (Fig. 11). Although it is small sample size, it does have sufficient power (>0.8) to be considered valid (67). These data confirmed that we did not introduce any bias by using isolated SCs in 2D cell culture and provided further support to the fact that SC-derived MBs and MTs accurately reflect the 3D tissue microenvironments.

Modeling the MEF2C regulation in CP

The reduced ability of CP SCs to generate new muscle fibers or repair may be linked to their muscle abnormalities. Previous studies have found that SCs taken from the muscles of individuals with cerebral palsy have a lower fusion index compared to those from typically developing children (16, 68–71). We confirmed that CP SCs had lower fusion indexes when compared to CN SCs. circNFIX KD cells also showed a similar phenotype, indicating that these cells have a reduced capacity to merge and form myotubes, which affects the development of sarcomeres (Fig. 12). This supports the functional role of circRNA in the disease.

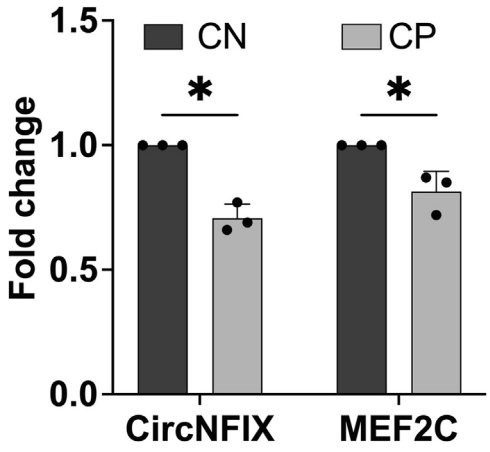

Figure 11. Average expression of circNFIX and MEF2C using total RNA isolated from skeletal muscle tissue of six individuals with CP normalized to the average expression in skeletal tissue of six CN samples as obtained by qRT-PCR. Experiment was performed in triplicate. Error bars indicate standard deviation. Significance (* = $p < 0.05$) was established using unpaired, two-tailed Student's *t* test. CN, control; CP, cerebral palsy; MEF2C, myocyte-specific enhancer factor 2C; NFIX, nuclear factor IX; qRT-PCR, quantitative reverse transcriptase PCR.

The circNFIX, miR373-3p, and MEF2C regulatory axis is crucial for muscle development. Our research has shown that circNFIX dysregulation continues throughout the differentiation process from myoblasts to myotubes, to finally the skeletal muscle tissue (Fig. 13*A*). We mapped the binding sites of miR-373-3p to circNFIX as well as MEF2C 3′ UTR and found that the binding site is fully complementary (Fig. 13*B*). We observed a significant decrease in the MEF2C protein level in myoblasts and myotubes, indicating that miR-373-3p is blocking the translation of MEF2C. Therefore, we suggest a MEF2C protein regulation model as shown in Figure 13*C*. Under normal physiological conditions, circNFIX competes with miR-373-3p for target sites, blocking its binding to MEF2C and resulting in a high expression of MEF2C protein (Fig. 13*C*). MEF2C is a transcription factor required for optimal expression of several genes including genes involved in sarcomere maturation (45–47). MEF2C has been linked to normal sarcomere length and function in healthy cells (65, 72). In cases of CP, the level of circNFIX is reduced which leads to an increase in the availability of miR-373-3p. This, in turn, effectively blocks the translation of MEF2C, leading to the production of less MEF2C protein by CP SC-MBs and SC-MTs. As a result, the expression of MEF2C targets is also reduced, which has the potential to alter sarcomere maturation as observed in CP patients.

Discussion

NFIX is a transcription factor involved in muscle and central nervous system development, as well as hematopoiesis. It has also been associated with muscular dystrophies, brain disorders, and various cancer types (73, 74). Moreover, six circRNAs have been reported to be produced from different exons

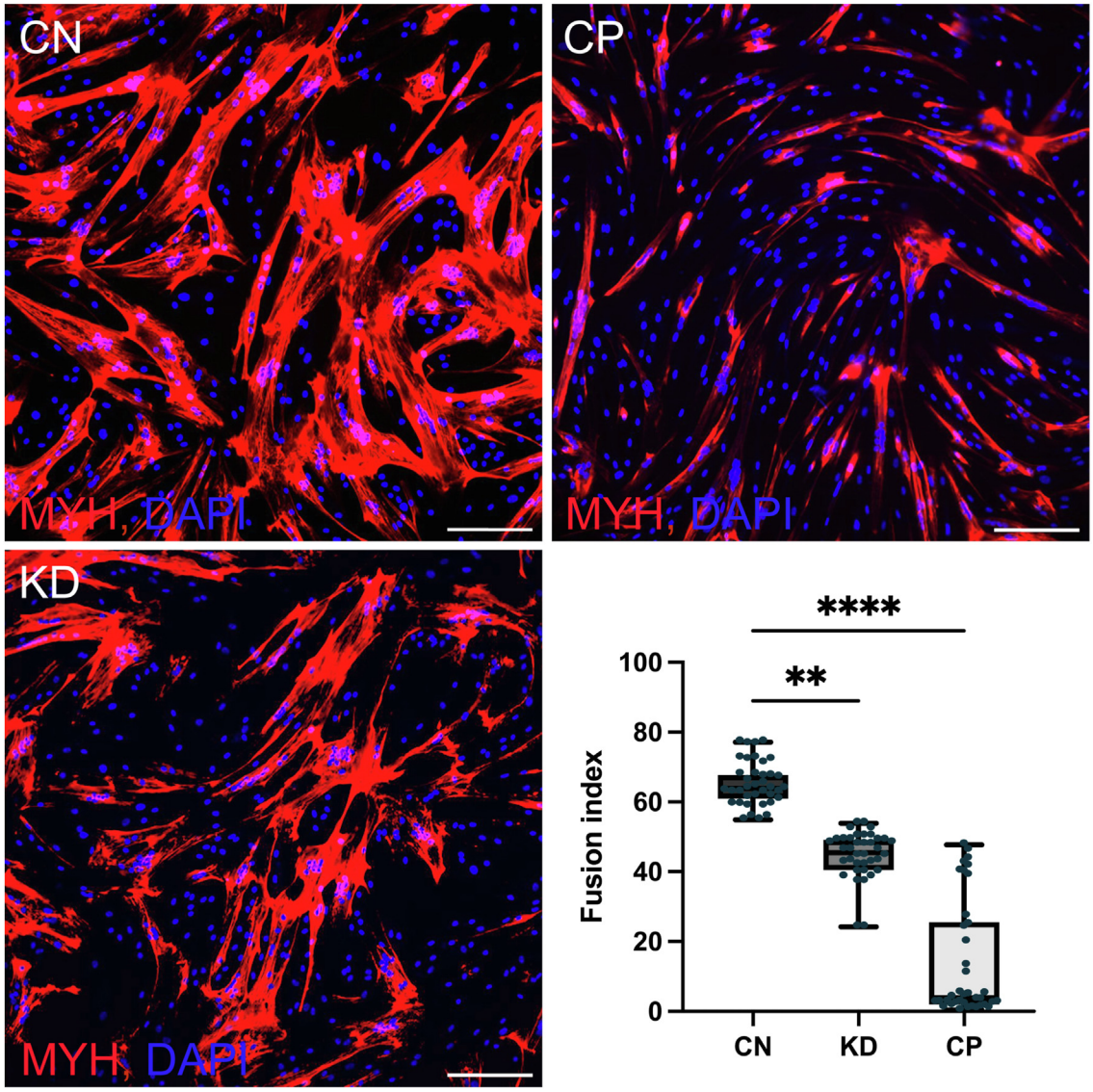

Figure 12. Representative images confirm that the fusion index of CP and KD is lower compared to CN. The staining of myosin heavy chain (MYH) depicts SC-MTs. The fusion index is the ratio of the number of nuclei (shown in *blue* with DAPI staining) inside a myotube (depicted in *red* with MYH staining) to the total number of nuclei per field of view. The whiskers represent the minimum and maximum values. Significance (** = $p < 0.01$, **** = $p < 0.0001$) was established using Kruskal–Wallis test. All experiments were performed in triplicate. The scale bar represents 10 μm. CN, control; CP, cerebral palsy; DAPI, 4′,6-diamidino-2-phenylindole; SC-MT, satellite cell-derived myotube.

of *NFIX* as per the databases of circRNAs (57). circNFIX is a critical regulatory circRNA that has been shown to play important functions in different biological contexts. The most well-studied circNFIX isoform (hsa-circ-0005660) is produced from exon 2 of *NFIX* and has been mostly investigated for its role in the cardiovascular system where it has been shown to sponge miRNAs as well as RNA binding proteins (38, 75, 76). Recent work by our collaborators also showed circNFIX regulates miR-204 function leading to regulation of MEF2C in myogenesis in mouse cell lines (37). However, most of this published work has been performed in mouse models, and there are no reports on the functional characterization of circRNAs in CP (77). Our analysis has found that circNFIX is a highly abundant circRNA in SC-derived myoblasts and myotubes. This is the first report of the use of circFISH for single-molecule resolution imaging of circNFIX that helped us to determine the localization and high expression level of circNFIX in SC-MBs from control *versus* those derived from the CP muscle. Since circRNAs usually function in their intracellular compartments, a shift toward nuclear localization of circNFIX in CP might indicate a molecular mechanism of sequestration of circNFIX in the nucleus and thus make it less available to act as competitive endogenous RNAs to miRNAs. This, coupled with the reduced expression, indicated a functional effect in reducing MEF2C protein levels in CP. The mechanism of this regulation is still elusive and warrants further studies to identify regulators of expression and localization of circNFIX in the SCs.

Although circNFIX is conserved between the mice and human, the circRNA:miRNA interactions are often species-

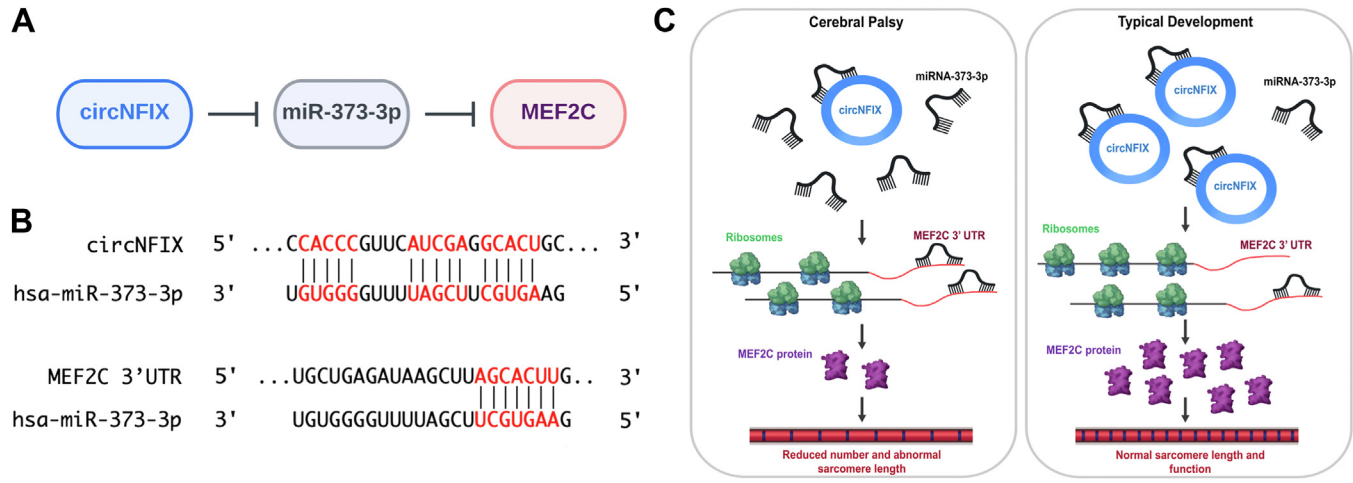

Figure 13. Model of the regulation of MEF2C expression in spastic cerebral palsy by circNFIX. *A*, the schematic of circRNA-miRNA-mRNA regulatory axis. *B*, binding sites for miR-373-3p in circNFIX and binding site of miR373-3p in the fragment 1 of MEF2C 3′UTR. *C*, hypothetical model for the functional role of circNFIX in muscle satellite cells. circRNA, circular RNA; DAPI, 4′,6-diamidino-2-phenylindole; MEF2C, myocyte-specific enhancer factor 2C; NFIX, nuclear factor IX.

specific and thus unlike in the mouse system, we did not find human circNFIX to interact and bind miR-204. Our work was therefore focused on identifying the regulatory axis of human circNFIX, particularly in the context of muscle SCs and sarcomere formation during myogenesis. Muscle SCs play critical roles in the normal development of muscles and are markedly affected during CP. Subjects with CP have a reduced number and function of muscle SCs, and poorly developed sarcomeres (7, 11). In this study, we found that circNFIX is reduced by 18%, 37%, and 29% in SC-MBs, SC-MTs and skeletal muscle tissue respectively from CP as compared to their corresponding controls. The MEF2C protein level was also significantly downregulated in CP as well as in circNFIX KD in the control cells, indicating that circNFIX is regulating the translation of MEF2C protein in SC-MBs, SC-MTs, and skeletal muscle tissue *via* miRNA sponging. MicroRNAs act as posttranscriptional regulators of mRNA targets by cleaving the mRNA and/or repressing the translation (78).

According to bioinformatic analysis and luciferase assays, we found that hsa-miR-373-3p can interact with circNFIX and MEF2C. At present, there is no report on the role of miR-373-3p in CP. Previous work indicated that miR-373 regulates cell growth and modulates cell migration and invasion and it plays important roles in different malignancies including breast cancer, prostate cancer, testicular germ cell tumor, and liver cancer (79). One report also found that overexpression of miR-373 decreased MEF2C expression and cell size of cultured mice cardiac myocytes (80).

In the present study, we found that MEF2C protein is downregulated in CP SC-MBs, SC-MTs, and skeletal muscle tissue. To the best of our knowledge, this is the first report on the regulation of MEF2C expression in CP. To further investigate the regulatory role of circNFIX in MEF2C translation, we used polysome fractionation and gene expression analysis. Polysome fractionation, facilitated by SEC, allowed for the separation of actively translating mRNAs associated with polysomes from those bound to ribosomal subunits (40S, 60S) or fully assembled solo ribosomes that undergo poor translation or remain untranslated (49). We discovered that MEF2C mRNA in CP and CN circNFIX KD samples exhibited a reduced association with polysomes in comparison to ribosomal subunits. Consequently, this decreased association with polysomes can explain the reduced translation of MEF2C protein. MEF2C expression contributes to sarcomere integrity and maintenance, by regulating the expression of sarcomere genes encoding structural proteins involved in the sarcomere architecture (81). Sarcomeres are responsible for muscle contraction, and dysfunction of sarcomeric proteins is associated with a variety of skeletal muscle diseases (82). It is known that muscles in CP have a reduced number of sarcomeres in series that are overstretched as compared to sarcomeres in typically developing children (83). It is hypothesized that the downregulation of MEF2C is responsible for the sarcomere pathology in CP. In mice, the loss of MEF2C disrupts sarcomere organization and causes defects in postnatal muscle maturation of skeletal muscle (46, 47). Furthermore, a previous study reported that circNFIX loss promotes de-differentiation and transient sarcomere disassembly in mouse adult cardiomyocytes (38).

Potthoff *et al.* (2007) discovered that skeletal muscle-specific deletion of *Mef2c* in mice displayed fragmented myofibers along the M-line, which are needed for maintaining sarcomere integrity. The study also revealed that the loss of MEF2C in skeletal muscle led to the downregulation of genes responsible for muscle contraction, particularly genes encoding cytoskeletal proteins. Among the downregulated genes were myomesins, myozenins, myotilin, actin, myosin, and muscle creatine kinase (46).

We evaluated the expression level of six known MEF2C target genes encoding myomesin, myozenin, and myotilin (45) and found that myomesins 1, 2, and 3, and myozenin 2 were downregulated in CP and KD compared to control myotubes. Myomesins aid in sarcomere stability, allowing it to return to its original state after contraction. Previous studies have shown

that myomesin 1 and myomesin 2 are directly activated by MEF2C, which binds to their promoters (46, 64, 84). Myomesin 1 is found in every muscle, while myomesin 2 and myomesin 3 are tissue-specific, present in the cardiac and fast skeletal muscle, and intermediate muscle and specific regions of the cardiac muscle, respectively (64). Myozenin 1 and 2 refer to Z-line interacting proteins and link calcineurin with the sarcomere by acting as stress sensors. Particularly, myozenin 2 has been reported to be regulated by MEF2A, which has a binding site in the proximal promoter, and it regulates muscle development through the calcineurin-NFAT signaling pathway. During skeletal muscle regeneration, MEF2C is expressed later than MEF2A (85). MEF2C is also known to target myozenin 2 and its lower expression may compromise the integrity of the Z-line and limit the sarcomeric contractile ability (72). On the other hand, myotilin is also necessary for sarcomere assembly and acts as an actin cross-linking protein (46). However, it has not been reported that MEF2C has a binding site in the myotilin promoter, and we did not find any significant change in myotilin expression level.

It has been reported that CP SCs have a reduced myogenic capacity. Many studies have shown that CP SCs have a lower fusion index and we confirmed those findings by staining the myotubes with anti-myosin heavy chain antibody (16, 68–71). We found that CP and circNFIX KD myotubes have a lower fusion index when compared to CN SC-MTs, which could explain why sarcomeres do not develop properly in CP, since cells are unable to fuse and generate myofibers. On the contrary, works by the Desloovere lab from Belgium have reported an increased fusion index in younger CP patients (15, 86, 87). Disparities in findings could be due to differences in SC isolation methods, age, and muscle heterogeneity but the general consensus in the field associates decreased fusion index in CP.

This is the first study to report a regulatory mechanism of MEF2C *via* circNFIX/miR-373-3p in CP. Although miRNA sponging is one of the most well-established roles of circRNAs, most of these "regulatory axes" do not bear clinical relevance due to a considerable gap between the copy number of circRNAs (often very low) and miRNA (often very high) in the cells and usually one or two binding sites for the miRNA in the circRNA (88). However, in the present study, we have a unique axis where the stoichiometry of copy number of circNFIX and miRNA are actually very much aligned to indicate a clinical relevance. The digital PCR and circFISH analysis identified an average of 60 copies of circNFIX in control SC-MTs while miR373-3p was found to be around 43 copies/cell. This indicates that even with a single confirmed binding site for miR373-3p, circNFIX would be able to have a significant sponging impact on the function of miR373-3p which is clearly evident by the results of the functional assays presented in this study.

As we established the circNFIX-mediated regulation of MEF2C protein, this mechanism *via* the miRNA sponging does not explain the observed reduction of MEF2C mRNA in CP and KD cells. This implies that circNFIX might be regulating the transcription of MEF2C *via* another mechanism. Furthermore, circNFIX might also interact with RNA binding proteins as shown previously in the case of its interaction with YBX-1 protein to regulate cardiac regeneration after myocardial infarction (38). Given the high level of expression of circNFIX in SC-MBs, SC-MTs, and skeletal muscle tissue, it would be interesting to explore its role in another regulatory axis. Ongoing work in our lab is also focused on finding other mechanisms of action of circNFIX as well as investigating whether circNFIX could be used as a diagnostic biomarker or therapeutic target.

Limitations of the study: This is the first report of functional characterization of circRNA function in CP. There is currently only one published report for the identification of circRNAs in blood from CP patients (89) and no reports on mechanism of action of circRNAs in CP. Therefore, future studies using a genome-wide analysis of circRNAs expressed in children with CP in muscle-derived SC-MBs as well as in blood are needed to obtain a complete profile of circRNA expression. The sample size for the study was small and heterogeneous. Future work with an expanded sample size separated by age, sex, and disease severity will provide more insights into subtleties of circRNA regulation in CP.

There is an unmet need for early diagnosis of CP that allows an early intervention to promote cognitive and motor development. Identification of regulatory circRNAs could very well fill this void in our understanding of the onset and progression of CP.

Experimental procedures

Human tissue samples, cells, and cell lines

The study was conducted according to the Declaration of Helsinki guidelines and approved by the IRB of Nemours (protocol number 687629). Muscle SCs were obtained from skeletal muscle biopsies collected during orthopedic surgeries of nine subjects for CP (with a diagnosis of spastic CP) and nine control subjects (with an idiopathic condition or injury but without any chromosomal or genetic disorder, degenerative neurological disease, or muscular dystrophy) at Nemours Children's Hospital, Delaware with approved IRBconsent/assent as described previously (90). Briefly, the biopsy material was digested with enzymes, and a double-immunomagnetic isolation approach was used to isolate SCs. The isolated SC-MBs were grown in proliferation medium containing Skeletal Muscle Growth Medium (ZenBio, catalog SKM-M) supplemented with 20% Qualified fetal bovine serum (Thermo Fisher Scientific, catalog # 26140079), 4 g/L of D-Glucose (Thermo Fisher Scientific, catalog # A2494001), 1 ng/ml of human bFGF (PeproTech, catalog # 100–18B), and 1% penicillin–streptomycin solution (Thermo Fisher Scientific, catalog # 15140122). The medium was exchanged every other day with fresh medium, and the cells were screened for presence of PAX7 and MYF5 expression using immunofluorescence before using for experiments. After SC-MBs reached 90 to 100% confluency, they were differentiated for 72 h in a low-serum medium. This medium consisted of high glucose Dulbecco's modified Eagle's medium (Thermo Fisher Scientific) that was supplemented with 2% horse serum (Thermo Fisher Scientific), 2% human insulin (Sigma-Aldrich) and 1% penicillin–streptomycin solution (Thermo Fisher Scientific, catalog # 15140122).

Cloning

For circNFIX silencing, the shRNA targeting the back splice junction of circNFIX was cloned into the pLKO.1-TRC cloning vector (Addgene, Plasmid # 10878) and transfected into HEK-293T cells for virus production along with helper plasmids. A scrambled shRNA sequence was also cloned into the pLKO.1-TRC cloning vector to use as a negative control. Viruses were harvested from HEK293T cells and added to a culture of proliferating SC cells. Selection of clones was done by adding 2 μg/ml puromycin (Gibco, A11138–03) to these cells 48 h after the transduction with viruses. The clones were validated using qRT-PCR. For luciferase assays, the empty psiCHECK2 plasmid and the plasmid, expressing different MEF2C 3′UTR fragments (psiCHECK2-MEF2C-3′UTR_F1, psiCHECK2-MEF2C-3′UTR_F2, and psiCHECK2-MEF2C-3′UTR_F3) were a kind gift from Dr Myriam Gorospe lab at National Institutes of Health (56). To validate the miRNA-mRNA interaction, ImiRP interface was used to generate a scrambled sequence that replace the hsa-miR-373-3p binding site in psiCHECK2-MEF2C-3′UTR_F1 (91) by using Q5 site-directed mutagenesis (New England Biolabs, M0491).

Quantitative reverse transcriptase PCR

SCs at 50% confluency were detached using trypsin, and total RNA was extracted using TRIzol extraction following the manufacturer's protocol (TRI Reagent, Sigma-Aldrich, T9424). The purity and concentrations of isolated RNA were measured using Nanodrop. Equal concentrations of RNA from control, CP, and CN NFIX KD and CN SCR cells were used to make complementary DNA (cDNA) using iScript Reverse Transcription Supermix (Bio-RAD, Hercules, 1708841). The obtained cDNA was used as a template to analyze expression of target genes as well as reference gene (GAPDH) using iTaq Universal SYBR Green Supermix (Bio-RAD 1725124) according to the manufacturer's protocol. circNFIX was amplified using divergent primers (37) and the linear RNAs were amplified using conventional convergent primers. Following Minimum Information for publication of Quantitative Real-Time Polymerase Chain Reaction Experiments guidelines, we also performed the normalization of RNA targets using 18S RNA and RNA polymerase III (Fig. S5). For miRNA expression analysis, total RNA was reverse transcribed using Mir-X miRNA First Strand Synthesis Kit following the manufacturer's protocol (Takara Bio, catalog # 638313). qRT-PCR was performed using the resulting cDNA, Mir-X miRNA qRT-PCR TB Green Kit (Takara Bio, catalog # 638314), and the specific forward primer for the miRNA along with the reverse common primer included in the kit. U6 forward and reverse primers included in the Mir-X miRNA First Strand Synthesis Kit were used as a normalization standard. For RNAse R treatment, total cellular RNA (2 μg) was incubated with 20U RNase R (Epicentre Technologies RNR07250) for 15 min at 37 °C, followed by cDNA synthesis and continuation with qRT-PCR as described above. Table S3 lists all the primers and antibodies used in the study.

Digital PCR

The copy number of circNFIX and hsa-miR-373-3p was identified by digital PCR (dPCR) using the Applied Biosystems QuantStudio Absolute Digital PCR (Thermo Fisher Scientific). The previously made cDNA was used as a template to calculate the copy number of circNFIX using Absolute Q DNA Digital PCR Master Mix (5X) according to the manufacturer's protocol (Thermo Fisher Scientific, A52490). A custom Taq-Man targeting the back-splice junction of circNFIX was designed and ordered from Thermo Fisher Scientific. For miRNA copy number identification, total RNA was reverse transcribed using Mir-X miRNA First Strand Synthesis Kit (Takara Bio, catalog # 638313) and dPCR was performed using the resulting cDNA, iTaq Universal SYBR Green Supermix (Bio-RAD 1725124), and the specific forward primer for the miRNA along with the reverse common primer included in the Mir-X miRNA First Strand Synthesis Kit.

circFISH, immunofluorescence, and image analysis

A set of circFISH probes called as PC probe set, was designed to target exon 2 of the *NFIX* and another set of probes called PL probe set was designed to target exon 11 of the *NFIX* gene so that colocalization of signals from PL and PC probe represent linear NFIX while signals from PC probe that do not colocalize with PL probe signal represent circNFIX as outlined in a recently published circFISH article from our lab (54). Briefly, the probes were ordered with a terminal -NH2 modification from LGC Bio search Technologies Inc. The obtained PC probes were pooled and labeled *en mass* with Texas red fluorophore while the PL probes were labeled with Cy5. The labeled fraction was purified using reverse phase HPLC. The proliferating SC-MBs from different cell lines were grown on gelatin coated glass coverslips. Upon 50% confluency, the cells were fixed, permeabilized and hybridized overnight with the labeled probes. The unbound probes were removed using exchanges of wash buffer. For RNAse R treatment, coverslips were incubated with 20U RNase R (Epicentre Technologies, RNR07250) for 4 h at 37 °C before proceeding to hybridization. For immunofluorescence, the permeabilized cells were incubated with blocking buffer, followed by overnight incubation at 4 °C with primary antibodies. The following day, another blocking step was performed followed by incubation with a secondary antibody for 1 h at room temperature and subsequent washing. For imaging, the cells were mounted with 4′,6-diamidino-2-phenylindole containing mounting medium and imaged using a 100X oil objective in Nikon TiE inverted fluorescence microscope equipped with a charge-coupled device Princeton Pixis 1024b camera. The images were acquired using Metamorph software (https://www.moleculardevices.com/products/cellular-imaging-systems/high-content-analysis/metamorph-microscopy) and analyzed using a custom-written program for spot counting in MATLAB (Mathworks Inc, USA). The corrected total cell fluorescence was calculated using ImageJ (https://imagej.net/ij/) (92) and the following formula was applied: corrected total cell fluorescence = integrated density–(area of selected cell × mean fluorescence of background readings) (93). The percentage of MEF2C positive nuclei was determined using the Fiji plugins

(https://fiji.sc/) (94) Colocalization Image Creator and Colocalization Object Counter, following the method described by Lunde and Glover (2020) (95). The list of antibodies and probes is provided in Tables S3 and S4, respectively.

Luciferase assay

The dual luciferase system from Promega was used for all luciferase experiments. SC-MBs from controls were transfected with either the psiCHECK2-empty plasmid or the psiCHECK2-MEF2C-3′UTR_F1, psiCHECK2-MEF2C-3′UTR_F2and psiCHECK2-MEF2C-3′UTR_F3 plasmid using Bio-T transfection reagent (Bioland Scientific LLC) using manufacturer's protocol. The cells were lysed 24 h after transfection using the Passive Lysis Buffer, (Promega, E194A) and the values of firefly and *Renilla* luciferase were read in a plate reader using the Dual-Luciferase Reagent Assay System (Promega, E1910) according to the manufacturer's protocol. For the miRNA mimic experiments, increasing concentrations of hsa-miR-373-3p mimic (Thermo Fisher Scientific, catalog #4464066) were included in the transfection with psiCHECK2-MEF2C-3′UTR_F1 in the CN and CP cells, respectively. The luciferase values were read 24 h post transfection as described above. The firefly luciferase (expressed constitutively) is used to normalize bioluminescence values obtained for *Renilla* luciferase which is expressed in fusion with the 3′UTR of MEF2C. To validate the interaction of miRNA-mRNA, a psiCHECK2-MEF2C-3′UTR_F1 missing the binding site of the miRNA and the WT construct were transfected along with miRNA mimics and subsequently lysed to perform the luciferase assay as described previously. In addition, a miRNA mimic negative control (Thermo Fisher Scientific, catalog #4464061) was included in the transfection along with the psiCHECK2-MEF2C-3′UTR_F1 to confirm that the observed effect in the previous experiments is indeed specific to hsa-miR-373-3p. The ratio of *Renilla* and *Firefly* was calculated, and the values for psiCHECK2-MEF2C-3′UTR_fragments were subtracted from the levels obtained in mock transfection. These values were then further subtracted from the values corresponding to the empty psiCHECK2. The final values were used to calculate fold change between CP and CN, or among the treatment or no treatment groups (mimic/negative control). Each experiment was repeated in triplicate and Student's t test was done to obtain p values.

Polysome fractionation

Polysome and ribosomal subunits were resolved from control, CP, and KD derived SC-MB cell extracts by SEC according to the protocol described by Yoshikawa *et al.*, 2018 (49). SC-MBs were grown to 60% confluency and treated with cycloheximide (100 µg/ml final concentration) (Sigma-Aldrich, C7698) for 10 min before performing lysis. The column used for polysome fractionation was Bio SEC-5, 5 µm particles, 2000 Å, 7.8 × 300 mm (Agilent Technologies, 5190–2541) using a Dionex Ultimate 3000 uHPLC system (Thermo Fisher Scientific). Subsequently, total RNA was extracted from each fraction using TRIzol extraction following the manufacturer's protocol (TRI Reagent, Sigma-Aldrich, T9424). Equal concentrations of RNA from control, CP, and CN NFIX KD were used to make cDNA using iScript Reverse Transcription Supermix (Bio-RAD, 1708841). The obtained cDNA was used as a template to analyze expression of MEF2C as well as reference gene (GAPDH) using iTaq Universal SYBR Green Supermix (Bio-RAD, 1725124) according to manufacturer's protocol.

Bioinformatic and statistical analyses

MiRNAs interacting with *circNFIX* and MEF2C 3′UTR fragment 1 were predicted using miRanda v3.3a, miRDB, and CircInteractome/TargetScan (57–60). Further comparison of the common miRNAs targeting *circNFIX* and *MEF2C* with miRTarBase v8 and Human miRNAs reported in miRNATissueAtlas2 identified high confidence miRNAs involved in the *circNFIX*-miRNA-MEF2C regulatory axis (62, 63). Each experiment was performed in triplicate and biological replicates. For fold changes in qRT-PCR, 2-delta delta Ct was calculated by normalization using a housekeeping gene. Fold change in luciferase experiments used empty and mock transfection for normalization. For imaging, at least 100 cells were counted to obtain average RNA counts or to quantify the protein signals. The error bars indicate either standard deviation or 95% confidence intervals indicated in each figure legend. p-values were obtained using Student's t test and Mann-Whitney test, and $p \leq 0.05$ was considered statistically significant. p-values were obtained using unpaired, two-tailed Student's t test and Kruskal–Wallis test, and $p \leq 0.05$ was considered statistically significant.

Data availability

The sequences of all the probes and primers used in the study are provided in the supplementary materials. The custom-written algorithms for image analysis in MATLAB can be made available upon a direct request to the corresponding author.

Supporting information—This article contains supporting information (54).

Acknowledgments—The authors would like to thank the Nemours Foundation, the Cerebral Palsy Program at Nemours, the Nemours Biomedical Research, and the Department of Pediatrics for institutional support of K. G. R., S. K. L., M. W. S., and R. E. A., as well as The Swank Foundation for their support to R. E. A. allowing the establishment of the neuro–orthopedic tissue repository at Nemours that provided samples for the work. Authors would like to thank Drs. Myriam Gorospe and Jennifer Martindale, laboratory of Genetics and Genomics at National Institute of Aging at NIH for their kind gift of luciferase plasmids and help with polysome fractionation.

Author contributions—B. R., P. H., K. G. R., S. K. L., T. S., and V. P. data curation; B. R., P. H., K. G. R., S. K. L., T. S., and M. B. methodology; B. R., P. H., T. S. and M. B. formal analysis; B. R., P. H., and T. S. visualization; B. R., P. H. and T. S. investigation; B.

R., P. H., K. G. R., V. P., R. E. A., and M. B. writing–review and editing; B. R., A. P., and M. B. validation; B. R. and M. B. writing–original draft; P. H., T. S., and A. P. software; V. P., R. E. A., and M. B. conceptualization; V. P., R. E. A., A. P., and M. B. supervision; V. P., R. E. A., A. P., M. W. S., and M. B. resources; V. P., R. E. A., and M. B. funding acquisition; R. E. A and M. B. project administration.

Funding and additional information—This work was supported by the National Science Foundation award 2244127 funds to M. B.; University of Delaware Research Foundation award to V.P., Delaware Bioscience Center for Advanced Technology funds to M. B. and V. P.; an American Academy for Cerebral Palsy and Developmental Medicine Pedal with Pete Foundation award, and programmatic funding from Nemours to R. E. A. The content is solely the responsibility of the authors and does not necessarily represent the official views of the National Institutes of Health.

Conflicts of interest—The authors declare that they have no conflicts of interest with the contents of this article.

Abbreviations—The abbreviations used are: cDNA, complementary DNA; circRNA, circular RNA; CP, cerebral palsy; dPCR, digital PCR; IRB, Institutional Review Board; MEF2C, myocyte-specific enhancer factor 2C; NFIX, nuclear factor IX; ncRNA, noncoding RNA; NMJ, neuromuscular junction; PB, polysome bound; PC, probe circular; PL, probe linear; qRT-PCR, quantitative reverse transcriptase PCR; SC, satellite cell; SC-MB, satellite cell-derived myoblast; SCR, scramble; SEC, size-exclusion chromatography; SC-MT, satellite cell-derived myotube.

References

1. Patel, D. R., Neelakantan, M., Pandher, K., and Merrick, J. (2020) Cerebral palsy in children: a clinical overview. *Transl Pediatr.* **9**, S125–S135
2. Lieber, R. L., and Fridén, J. (2002) Spasticity causes a fundamental rearrangement of muscle-joint interaction. *Muscle Nerve* **25**, 265–270
3. Accardo, P., and Capute, A. (2008) *Capute & Accardo's Neurodevelopmental Disabilities in Infancy and Childhood*, 3er ed Edition, Paul H. Brookes, Baltimore, MD
4. Mockford, M., and Caulton, J. M. (2010) The pathophysiological basis of weakness in children with cerebral palsy. *Pediatr. Phys. Ther.* **22**, 222–233
5. Sankar, C., and Mundkur, N. (2005) Cerebral palsy-definition, classification, etiology and early diagnosis. *Indian J. Pediatr.* **72**, 865–868
6. Chin, E. M., Gwynn, H. E., Robinson, S., and Hoon, A. H. (2020) Principles of medical and surgical treatment of cerebral palsy. *Neurol. Clin.* **38**, 397–416
7. Graham, H. K., Rosenbaum, P., Paneth, N., Dan, B., Lin, J. P., Damiano, D. L., *et al.* (2016) Cerebral palsy. *Nat. Rev. Dis. Primers* **2**, 15082
8. Dayanidhi, S., and Lieber, R. L. (2014) Skeletal muscle satellite cells: mediators of muscle growth during development and implications for developmental disorders. *Muscle Nerve* **50**, 723–732
9. Lepper, C., Partridge, T. A., and Fan, C. M. (2011) An absolute requirement for Pax7-positive satellite cells in acute injury-induced skeletal muscle regeneration. *Development* **138**, 3639–3646
10. Smith, L. R., Chambers, H. G., and Lieber, R. L. (2013) Reduced satellite cell population may lead to contractures in children with cerebral palsy. *Dev. Med. Child Neurol.* **55**, 264–270
11. Howard, J. J., and Herzog, W. (2021) Skeletal muscle in cerebral palsy: from belly to myofibril. *Front. Neurol.* **12**, 620852
12. Liu, W., Wei-LaPierre, L., Klose, A., Dirksen, R. T., and Chakkalakal, J. V. (2015) Inducible depletion of adult skeletal muscle stem cells impairs the regeneration of neuromuscular junctions. *Elife* **4**, e09221
13. Liu, W., Klose, A., Forman, S., Paris, N. D., Wei-LaPierre, L., Cortés-Lopéz, M., *et al.* (2017) Loss of adult skeletal muscle stem cells drives age-related neuromuscular junction degeneration. *Elife* **6**, e26464
14. Robinson, K. G., and Akins, R. E. (2019) *Neuromuscular Junction Changes in Spastic Cerebral Palsy*, Springer International Publishing, Cham, Switzerland
15. Corvelyn, M., De Beukelaer, N., Duelen, R., Deschrevel, J., Van Campenhout, A., Prinsen, S., *et al.* (2020) Muscle microbiopsy to delineate stem cell involvement in young patients: a novel approach for children with cerebral palsy. *Front. Physiol.* **11**, 945
16. Domenighetti, A. A., Mathewson, M. A., Pichika, R., Sibley, L. A., Zhao, L., Chambers, H. G., *et al.* (2018) Loss of myogenic potential and fusion capacity of muscle stem cells isolated from contractured muscle in children with cerebral palsy. *Am. J. Physiol. Cell Physiol.* **315**, C247–C257
17. Ballarino, M., Morlando, M., Fatica, A., and Bozzoni, I. (2016) Non-coding RNAs in muscle differentiation and musculoskeletal disease. *J. Clin. Invest.* **126**, 2021–2030
18. Liu, Y., Gu, X., Liu, H., Li, Z., Wang, Z., Zhu, Z., *et al.* (2020) New insight of circular RNAs in human musculoskeletal diseases. *DNA Cell Biol.* **39**, 1938–1947
19. Chen, G., Tang, W., Wang, S., Long, C., He, X., Yang, D., *et al.* (2021) Promising diagnostic and therapeutic circRNAs for skeletal and chondral disorders. *Int. J. Biol. Sci.* **17**, 1428–1439
20. Memczak, S., Jens, M., Elefsinioti, A., Torti, F., Krueger, J., Rybak, A., *et al.* (2013) Circular RNAs are a large class of animal RNAs with regulatory potency. *Nature* **495**, 333–338
21. Hsu, M. T., and Coca-Prados, M. (1979) Electron microscopic evidence for the circular form of RNA in the cytoplasm of eukaryotic cells. *Nature* **280**, 339–340
22. Cocquerelle, C., Daubersies, P., Majérus, M. A., Kerckaert, J. P., and Bailleul, B. (1992) Splicing with inverted order of exons occurs proximal to large introns. *EMBO J.* **11**, 1095–1098
23. Cocquerelle, C., Mascrez, B., Hétuin, D., and Bailleul, B. (1993) Mis-splicing yields circular RNA molecules. *FASEB J.* **7**, 155–160
24. Vicens, Q., and Westhof, E. (2014) Biogenesis of circular RNAs. *Cell* **159**, 13–14
25. Palazzo, A. F., and Lee, E. S. (2015) Non-coding RNA: what is functional and what is junk? *Front. Genet.* **6**, 2
26. Nigro, J. M., Cho, K. R., Fearon, E. R., Kern, S. E., Ruppert, J. M., Oliner, J. D., *et al.* (1991) Scrambled exons. *Cell* **64**, 607–613
27. Granados-Riveron, J. T., and Aquino-Jarquin, G. (2016) The complexity of the translation ability of circRNAs. *Biochim. Biophys. Acta* **1859**, 1245–1251
28. Pamudurti, N. R., Bartok, O., Jens, M., Ashwal-Fluss, R., Stottmeister, C., Ruhe, L., *et al.* (2017) Translation of CircRNAs. *Mol. Cell* **66**, 9–21.e27
29. Hansen, T. B., Jensen, T. I., Clausen, B. H., Bramsen, J. B., Finsen, B., Damgaard, C. K., *et al.* (2013) Natural RNA circles function as efficient microRNA sponges. *Nature* **495**, 384–388
30. Li, Z., Huang, C., Bao, C., Chen, L., Lin, M., Wang, X., *et al.* (2015) Exon-intron circular RNAs regulate transcription in the nucleus. *Nat. Struct. Mol. Biol.* **22**, 256–264
31. Qu, S., Yang, X., Li, X., Wang, J., Gao, Y., Shang, R., *et al.* (2015) Circular RNA: a new star of noncoding RNAs. *Cancer Lett.* **365**, 141–148
32. Abu, N., and Jamal, R. (2016) Circular RNAs as promising biomarkers: a mini-review. *Front. Physiol.* **7**, 355
33. Rybak-Wolf, A., Stottmeister, C., Glažar, P., Jens, M., Pino, N., Giusti, S., *et al.* (2015) Circular RNAs in the mammalian brain are highly abundant, conserved, and dynamically expressed. *Mol. Cell* **58**, 870–885
34. Yang, Z., He, T., and Chen, Q. (2021) The roles of CircRNAs in regulating muscle development of livestock animals. *Front. Cell Dev. Biol.* **9**, 619329
35. Zheng, S., Zhang, X., Odame, E., Xu, X., Chen, Y., Ye, J., *et al.* (2021) CircRNA-protein interactions in muscle development and diseases. *Int. J. Mol. Sci.* **22**, 3262
36. Cui, X., Dong, Y., Li, M., Wang, X., Jiang, M., Yang, W., *et al.* (2020) A circular RNA from NFIX facilitates oxidative stress-induced H9c2 cells apoptosis. *In Vitro Cell Dev. Biol. Anim.* **56**, 715–722
37. Das, A., Shyamal, S., Sinha, T., Mishra, S. S., and Panda, A. C. (2021) Identification of potential circRNA-microRNA-mRNA regulatory network in skeletal muscle. *Front. Mol. Biosci.* **8**, 762185

38. Huang, S., Li, X., Zheng, H., Si, X., Li, B., Wei, G., *et al.* (2019) Loss of super-enhancer-regulated circRNA nfix induces cardiac regeneration after myocardial infarction in adult mice. *Circulation* **139**, 2857–2876
39. Lu, J., Zhu, Y., Qin, Y., and Chen, Y. (2020) CircNFIX acts as a miR-212-3p sponge to enhance the malignant progression of non-small cell lung cancer by up-regulating ADAM10. *Cancer Manag. Res.* **12**, 9577–9587
40. Cheng, J., Nie, D., Li, B., Gui, S., Li, C., Zhang, Y., *et al.* (2021) CircNFIX promotes progression of pituitary adenoma *via* CCNB1 by sponging miR-34a -5p. *Mol. Cell Endocrinol.* **525**, 111140
41. Xiao, E., Zhang, D., Zhan, W., Yin, H., Ma, L., Wei, J., *et al.* (2021) circNFIX facilitates hepatocellular carcinoma progression by targeting miR-3064-5p/HMGA2 to enhance glutaminolysis. *Am. J. Transl. Res.* **13**, 8697–8710
42. Xu, H., Zhang, Y., Qi, L., Ding, L., Jiang, H., and Yu, H. (2018) NFIX circular RNA promotes glioma progression by regulating miR-34a-5p *via* notch signaling pathway. *Front. Mol. Neurosci.* **11**, 225
43. Ivanov, Y. D., Malsagova, K. A., Popov, V. P., Pleshakova, T. O., Kozlov, A. F., Galiullin, R. A., *et al.* (2021) Nanoribbon-based electronic detection of a glioma-associated circular miRNA. *Biosensors (Basel)* **11**, 237
44. Bienvenu, T., Diebold, B., Chelly, J., and Isidor, B. (2013) Refining the phenotype associated with MEF2C point mutations. *Neurogenetics* **14**, 71–75
45. Ow, J. R., Palanichamy Kala, M., Rao, V. K., Choi, M. H., Bharathy, N., and Taneja, R. (2016) G9a inhibits MEF2C activity to control sarcomere assembly. *Sci. Rep.* **6**, 34163
46. Potthoff, M. J., Arnold, M. A., McAnally, J., Richardson, J. A., Bassel-Duby, R., and Olson, E. N. (2007) Regulation of skeletal muscle sarcomere integrity and postnatal muscle function by Mef2c. *Mol. Cell Biol.* **27**, 8143–8151
47. Anderson, C. M., Hu, J., Barnes, R. M., Heidt, A. B., Cornelissen, I., and Black, B. L. (2015) Myocyte enhancer factor 2C function in skeletal muscle is required for normal growth and glucose metabolism in mice. *Skelet Muscle* **5**, 7
48. Suzuki, H., Zuo, Y., Wang, J., Zhang, M. Q., Malhotra, A., and Mayeda, A. (2006) Characterization of RNase R-digested cellular RNA source that consists of lariat and circular RNAs from pre-mRNA splicing. *Nucleic Acids Res.* **34**, e63
49. Yoshikawa, H., Larance, M., Harney, D. J., Sundaramoorthy, R., Ly, T., Owen-Hughes, T., *et al.* (2018) Efficient analysis of mammalian polysomes in cells and tissues using Ribo Mega-SEC. *Elife* **7**, e36530
50. Bassett, A. R., Akhtar, A., Barlow, D. P., Bird, A. P., Brockdorff, N., Duboule, D., *et al.* (2014) Considerations when investigating lncRNA function *in vivo*. *Elife* **3**, e03058
51. Ivanov, A., Memczak, S., Wyler, E., Torti, F., Porath, H. T., Orejuela, M. R., *et al.* (2015) Analysis of intron sequences reveals hallmarks of circular RNA biogenesis in animals. *Cell Rep.* **10**, 170–177
52. Batish, M., Raj, A., and Tyagi, S. (2011) Single molecule imaging of RNA in situ. *Methods Mol. Biol.* **714**, 3–13
53. Markey, F. B., Ruezinsky, W., Tyagi, S., and Batish, M. (2014) Fusion FISH imaging: single-molecule detection of gene fusion transcripts in situ. *PLoS One* **9**, e93488
54. Koppula, A., Abdelgawad, A., Guarnerio, J., Batish, M., and Parashar, V. (2022) CircFISH: a novel method for the simultaneous imaging of linear and circular RNAs. *Cancers (Basel)* **14**, 428
55. Xiao, M. S., and Wilusz, J. E. (2019) An improved method for circular RNA purification using RNase R that efficiently removes linear RNAs containing G-quadruplexes or structured 3' ends. *Nucleic Acids Res.* **47**, 8755–8769
56. Yang, J. H., Chang, M. W., Pandey, P. R., Tsitsipatis, D., Yang, X., Martindale, J. L., *et al.* (2020) Interaction of OIP5-AS1 with MEF2C mRNA promotes myogenic gene expression. *Nucleic Acids Res.* **48**, 12943–12956
57. Dudekula, D. B., Panda, A. C., Grammatikakis, I., De, S., Abdelmohsen, K., and Gorospe, M. (2016) CircInteractome: a web tool for exploring circular RNAs and their interacting proteins and microRNAs. *RNA Biol.* **13**, 34–42
58. McGeary, S. E., Lin, K. S., Shi, C. Y., Pham, T. M., Bisaria, N., Kelley, G. M., *et al.* (2019) The biochemical basis of microRNA targeting efficacy. *Science* **366**. https://doi.org/10.1126/science.aav1741
59. Chen, Y., and Wang, X. (2020) miRDB: an online database for prediction of functional microRNA targets. *Nucleic Acids Res.* **48**, D127–D131
60. Enright, A. J., John, B., Gaul, U., Tuschl, T., Sander, C., and Marks, D. S. (2003) MicroRNA targets in Drosophila. *Genome Biol.* **5**, R1
61. Lewis, B. P., Burge, C. B., and Bartel, D. P. (2005) Conserved seed pairing, often flanked by adenosines, indicates that thousands of human genes are microRNA targets. *Cell* **120**, 15–20
62. Huang, H. Y., Lin, Y. C., Cui, S., Huang, Y., Tang, Y., Xu, J., *et al.* (2022) miRTarBase update 2022: an informative resource for experimentally validated miRNA-target interactions. *Nucleic Acids Res.* **50**, D222–D230
63. Keller, A., Gröger, L., Tschernig, T., Solomon, J., Laham, O., Schaum, N., *et al.* (2022) miRNATissueAtlas2: an update to the human miRNA tissue atlas. *Nucleic Acids Res.* **50**, D211–D221
64. Lamber, E. P., Guicheney, P., and Pinotsis, N. (2022) The role of the M-band myomesin proteins in muscle integrity and cardiac disease. *J. Biomed. Sci.* **29**, 18
65. Liu, N., Nelson, B. R., Bezprozvannaya, S., Shelton, J. M., Richardson, J. A., Bassel-Duby, R., *et al.* (2014) Requirement of MEF2A, C, and D for skeletal muscle regeneration. *Proc. Natl. Acad. Sci. U. S. A.* **111**, 4109–4114
66. Yu, D., Cai, Z., Li, D., Zhang, Y., He, M., Yang, Y., *et al.* (2021) Myogenic differentiation of stem cells for skeletal muscle regeneration. *Stem Cells Int.* **2021**, 8884283
67. Cohen, J. (1988) *Statistical Power Analysis for Behavioral Sciences*, Second Edition Edition, Routledge, Oxfordshire, England
68. Sibley, L. A., Broda, N., Gross, W. R., Menezes, A. F., Embry, R. B., Swaroop, V. T., *et al.* (2021) Differential DNA methylation and transcriptional signatures characterize impairment of muscle stem cells in pediatric human muscle contractures after brain injury. *FASEB J.* **35**, e21928
69. Kahn, R. E., Krater, T., Larson, J. E., Encarnacion, M., Karakostas, T., Patel, N. M., *et al.* (2023) Resident muscle stem cell myogenic characteristics in postnatal muscle growth impairments in children with cerebral palsy. *Am. J. Physiol. Cell Physiol.* **324**, C614–C631
70. Lieber, R. L., and Domenighetti, A. A. (2021) Commentary: muscle microbiopsy to delineate stem cell involvement in young patients: a novel approach for children with cerebral palsy. *Front. Physiol.* **12**, 642366
71. Loomis, T., Kulkarni, V. A., Villalba, M., Davids, J. R., Leach, J. K., and Smith, L. R. (2024) Muscle satellite cells and fibro-adipogenic progenitors from muscle contractures of children with cerebral palsy have impaired regenerative capacity. *Dev. Med. Child Neurol.* https://doi.org/10.1111/dmcn.16006
72. Shum, A. M., Mahendradatta, T., Taylor, R. J., Painter, A. B., Moore, M. M., Tsoli, M., *et al.* (2012) Disruption of MEF2C signaling and loss of sarcomeric and mitochondrial integrity in cancer-induced skeletal muscle wasting. *Aging (Albany NY)* **4**, 133–143
73. Piper, M., Gronostajski, R., and Messina, G. (2019) Nuclear factor one X in development and disease. *Trends Cell Biol* **29**, 20–30
74. Ribeiro, V., Martins, S. G., Lopes, A. S., Thorsteinsdóttir, S., Zilhão, R., and Carlos, A. R. (2023) NFIXing cancer: the role of NFIX in oxidative stress response and cell fate. *Int. J. Mol. Sci.* **24**. https://doi.org/10.3390/ijms24054293
75. Pan, J., Xu, Z., Guo, G., Xu, C., Song, Z., Li, K., *et al.* (2021) Circ_nuclear factor I X (circNfix) attenuates pressure overload-induced cardiac hypertrophy *via* regulating miR-145-5p/ATF3 axis. *Bioengineered* **12**, 5373–5385
76. Wang, X., Sun, Q., and Hu, W. (2021) Carvedilol protects against the H2O2-induced cell damages in rat myoblasts by regulating the circ_NFIX/miR-125b-5p/TLR4 signal Axis. *J. Cardiovasc. Pharmacol.* **78**, 604–614
77. Romero, B., Robinson, K. G., Batish, M., and Akins, R. E. (2021) An emerging role for epigenetics in cerebral palsy. *J. Pers Med.* **11**, 1187
78. Catalanotto, C., Cogoni, C., and Zardo, G. (2016) MicroRNA in control of gene expression: an overview of nuclear functions. *Int. J. Mol. Sci.* **17**, 1712
79. Wei, F., Cao, C., Xu, X., and Wang, J. (2015) Diverse functions of miR-373 in cancer. *J. Transl Med.* **13**, 162

80. Shen, E., Diao, X., Wang, X., Chen, R., and Hu, B. (2011) MicroRNAs involved in the mitogen-activated protein kinase cascades pathway during glucose-induced cardiomyocyte hypertrophy. *Am. J. Pathol.* **179**, 639–650
81. Nath, S. R., Lieberman, M. L., Yu, Z., Marchioretti, C., Jones, S. T., Danby, E. C. E., *et al.* (2020) MEF2 impairment underlies skeletal muscle atrophy in polyglutamine disease. *Acta Neuropathol.* **140**, 63–80
82. Laing, N. G., and Nowak, K. J. (2005) When contractile proteins go bad: the sarcomere and skeletal muscle disease. *Bioessays* **27**, 809–822
83. Handsfield, G. G., Williams, S., Khuu, S., Lichtwark, G., and Stott, N. S. (2022) Muscle architecture, growth, and biological Remodelling in cerebral palsy: a narrative review. *BMC Musculoskelet. Disord.* **23**, 233
84. Lange, S., Pinotsis, N., Agarkova, I., and Ehler, E. (2020) The M-band: the underestimated part of the sarcomere. *Biochim. Biophys. Acta Mol. Cell Res.* **1867**, 118440
85. Wang, Y. N., Yang, W. C., Li, P. W., Wang, H. B., Zhang, Y. Y., and Zan, L. S. (2018) Myocyte enhancer factor 2A promotes proliferation and its inhibition attenuates myogenic differentiation *via* myozenin 2 in bovine skeletal muscle myoblast. *PLoS One* **13**, e0196255
86. Corvelyn, M., Meirlevede, J., Deschrevel, J., Huyghe, E., De Wachter, E., Gayan-Ramirez, G., *et al.* (2023) Ex vivo adult stem cell characterization from multiple muscles in ambulatory children with cerebral palsy during early development of contractures. *Differentiation* **133**, 25–39
87. Noë, S., Corvelyn, M., Willems, S., Costamagna, D., Aerts, J. M., Van Campenhout, A., *et al.* (2022) The Myotube Analyzer: how to assess myogenic features in muscle stem cells. *Skelet Muscle* **12**, 12
88. Hoque, P., Romero, B., Akins, R. E., and Batish, M. (2023) Exploring the multifaceted biologically relevant roles of circRNAs: from regulation, translation to biomarkers. *Cells* **12**. https://doi.org/10.3390/cells12242813
89. Hu, Y., Bian, X., Wu, C., Wang, Y., Wu, Y., Gu, X., *et al.* (2022) Genome-wide analysis of circular RNAs and validation of hsa_circ_0086354 as a promising biomarker for early diagnosis of cerebral palsy. *BMC Med. Genomics* **15**, 13
90. Robinson, K. G., Marsh, A. G., Lee, S. K., Hicks, J., Romero, B., Batish, M., *et al.* (2022) DNA methylation analysis reveals distinct patterns in satellite cell-derived myogenic progenitor cells of subjects with spastic cerebral palsy. *J. Pers. Med.* **12**. https://doi.org/10.3390/jpm12121978
91. Ryan, B. C., Werner, T. S., Howard, P. L., and Chow, R. L. (2016) ImiRP: a computational approach to microRNA target site mutation. *BMC Bioinformatics* **17**, 190
92. Schneider, C. A., Rasband, W. S., and Eliceiri, K. W. (2012) NIH Image to ImageJ: 25 years of image analysis. *Nat. Methods* **9**, 671–675
93. McCloy, R. A., Rogers, S., Caldon, C. E., Lorca, T., Castro, A., and Burgess, A. (2014) Partial inhibition of Cdk1 in G 2 phase overrides the SAC and decouples mitotic events. *Cell Cycle* **13**, 1400–1412
94. Schindelin, J., Arganda-Carreras, I., Frise, E., Kaynig, V., Longair, M., Pietzsch, T., *et al.* (2012) Fiji: an open-source platform for biological-image analysis. *Nat. Methods* **9**, 676–682
95. Lunde, A., and Glover, J. C. (2020) A versatile toolbox for semi-automatic cell-by-cell object-based colocalization analysis. *Sci. Rep.* **10**, 19027